Article

Current Biology

RDH12 allows cone photoreceptors to regenerate opsin visual pigments from a chromophore precursor to escape competition with rods

Highlights

- ZCRDH is an 11-*cis*-retinol-oxidase present in zebrafish cone inner segments
- *Zcrdh*-mutant zebrafish exhibit impaired synthesis of visual chromophore
- *Zcrdh*-mutant cones cannot regenerate visual pigments from 11-*cis*-retinol
- The mammalian ortholog of ZCRDH is RDH12

Authors

Joanna J. Kaylor, Rikard Frederiksen, Christina K. Bedrosian, ..., Alapakkam P. Sampath, Gordon L. Fain, Gabriel H. Travis

Correspondence

travis@jsei.ucla.edu

In brief

In daylight, cone visual pigments regenerate by a photic visual cycle in Müller cells of the retina. The photic visual cycle provides chromophore precursor to cones, which convert it to visual chromophore. Kaylor et al. identify the protein responsible for this conversion in zebrafish retinas and show that the mammalian ortholog is RDH12.

Kaylor et al., 2024, Current Biology *34*, 1–12
August 5, 2024
https://doi.org/10.1016/j.cub.2024.06.031

CellPress

Current Biology

CellPress
OPEN ACCESS

Article

RDH12 allows cone photoreceptors to regenerate opsin visual pigments from a chromophore precursor to escape competition with rods

Joanna J. Kaylor,[1] Rikard Frederiksen,[1] Christina K. Bedrosian,[1] Melody Huang,[1] David Stennis-Weatherspoon,[1] Theodore Huynh,[1] Tiffany Ngan,[1] Varsha Mulamreddy,[1] Alapakkam P. Sampath,[1] Gordon L. Fain,[1] and Gabriel H. Travis[1,2,3,*]

[1]University of California, Los Angeles, David Geffen School of Medicine, Department of Ophthalmology, 405 Hilgard Avenue, Los Angeles, CA 90095, USA

[2]University of California Los Angeles, Department of Biological Chemistry, 405 Hilgard Avenue, Los Angeles, CA 90095, USA

[3]Lead contact

*Correspondence: travis@jsei.ucla.edu

https://doi.org/10.1016/j.cub.2024.06.031

SUMMARY

Capture of a photon by an opsin visual pigment isomerizes its 11-*cis*-retinaldehyde (11cRAL) chromophore to all-*trans*-retinaldehyde (atRAL), which subsequently dissociates. To restore light sensitivity, the unliganded apo-opsin combines with another 11cRAL to make a new visual pigment. Two enzyme pathways supply chromophore to photoreceptors. The canonical visual cycle in retinal pigment epithelial cells supplies 11cRAL at low rates. The photic visual cycle in Müller cells supplies cones with 11-*cis*-retinol (11cROL) chromophore precursor at high rates. Although rods can only use 11cRAL to regenerate rhodopsin, cones can use 11cRAL or 11cROL to regenerate cone visual pigments. We performed a screen in zebrafish retinas and identified ZCRDH as a candidate for the enzyme that converts 11cROL to 11cRAL in cone inner segments. Retinoid analysis of eyes from *Zcrdh*-mutant zebrafish showed reduced 11cRAL and increased 11cROL levels, suggesting impaired conversion of 11cROL to 11cRAL. By microspectrophotometry, isolated *Zcrdh*-mutant cones lost the capacity to regenerate visual pigments from 11cROL. ZCRDH therefore possesses all predicted properties of the cone 11cROL dehydrogenase. The human protein most similar to ZCRDH is RDH12. By immunocytochemistry, ZCRDH was abundantly present in cone inner segments, similar to the reported distribution of RDH12. Finally, RDH12 was the only mammalian candidate protein to exhibit 11cROL-oxidase catalytic activity. These observations suggest that RDH12 in mammals is the functional ortholog of ZCRDH, which allows cones, but not rods, to regenerate visual pigments from 11cROL provided by Müller cells. This capacity permits cones to escape competition from rods for visual chromophore in daylight-exposed retinas.

INTRODUCTION

Visual perception in vertebrates begins with the capture of a photon in the outer segments (OSs) of retinal photoreceptor neurons by an opsin visual pigment. The huge dynamic range (>10^8-fold) of the visual systems in humans and other animals is largely due to the specialization of photoreceptors into high-sensitivity rods and low-sensitivity cones, with cones in many species providing color vision at high temporal and spatial resolution. Rhodopsin and the cone opsins are members of the G protein-coupled receptor superfamily. The ligand for these proteins is the chromophore, 11-*cis*-retinaldehyde (11cRAL), which is covalently coupled to a Lys residue as a protonated Schiff base. Absorption of a photon by an opsin pigment isomerizes the 11cRAL to all-*trans*-retinaldehyde (atRAL), which activates the pigment and thereby visual transduction. After a brief period of activation, the pigment decays, or bleaches, to yield unliganded (apo-) opsin and free atRAL. Light sensitivity is restored to the apo-opsin when it combines with another 11cRAL to form a new visual pigment. Conversion of atRAL to 11cRAL is carried out by two multi-step enzyme pathways called visual cycles in the cells of the retinal pigment epithelium (RPE) and Müller glial cells of the neural retina.

The product of the canonical visual cycle in RPE cells is 11cRAL, which is released into the extracellular space and taken up by photoreceptors to regenerate rod and cone visual pigments. However, the maximum turnover rate of Rpe65 is much slower than the estimated rate of visual-pigment photoisomerization in a daylight-exposed eye.[1] To sustain light sensitivity, the rate of 11cRAL synthesis must keep up with the rate of chromophore consumption. Because vision persists indefinitely under daylight conditions, these findings imply the existence of a second visual cycle that supports regeneration of cone-opsin pigments.

Earlier studies provided clues about this cone pathway. Cones, but not rods, recovered sensitivity following light

Please cite this article in press as: Kaylor et al., RDH12 allows cone photoreceptors to regenerate opsin visual pigments from a chromophore precursor to escape competition with rods, Current Biology (2024), https://doi.org/10.1016/j.cub.2024.06.031

exposure in retinas separated from the RPE,[2–4] indicating that all required components of the cone visual cycle are present within the neural retina. Müller glial cells were shown to be the likely site of this pathway because multiple retinoid-processing proteins are present in Müller cells.[5–9] Further, primary cultured Müller cells took up atROL and released 11cROL in the culture medium.[10] Finally, the treatment of isolated retinas with the glial toxin, α-aminoadipic acid,[11] abolished recovery of cone sensitivity in isolated retinas.[4] All of the retinoid-processing proteins in Müller cells are also present in RPE cells. However, the three enzymes of the canonical visual cycle (LRAT, Rpe65, and RDH5), although present in the RPE, are not present in Müller glia or any other cells of the neural retina.[6,12] Accordingly, by studying retinas separate from the RPE, the cone visual cycle can be investigated without confounding activities of the canonical visual cycle.

Many studies characterizing the visual cycles were performed in mice. However, the mouse is a poor model system to study cones biochemically because rods comprise ~97% of photoreceptors in mouse retinas, whereas cones comprise only ~3%. Additionally, mice are nocturnal animals that use cones differently from animals active in daylight. For example, the ultraviolet (UV)-sensitive cones in the mouse retina detect shadows, such as those of predators, against the night sky, dimly lit by scattered UV radiation. These cones function more as UV-sensitive rods in mice, imposing only a tiny burden on the visual cycle. The cone visual cycle, which maintains photosensitivity during exposure to daylight, is therefore scarcely needed in the mouse retina. Although cones are diffusely spread throughout the mouse retina, they are concentrated in the central human retina. In fact, the fovea at the optical center of the human retina is populated exclusively with slender cones that operate at high temporal frequency, enabling us to read fine print and track fast-moving objects in bright light. To perform these functions, foveal cones require a rapid resupply of visual chromophore and are therefore dependent on the cone visual cycle in Müller cells. Given the high degree of evolutionary conservation of photoreceptors across vertebrate species,[13] we sought a more appropriate model system to identify an unknown protein in cones. Besides their genetic tractability, adult zebrafish have cone-dominant retinas (~60%), are active during daylight, and use their cones to hunt for food. Zebrafish cones therefore operate under light conditions similar to cones in humans and other diurnal species.

The product of the cone visual cycle in Müller cells is the chromophore precursor, 11cROL,[10,14,15] which is used by cones to regenerate cone-opsin pigments.[16,17] In contrast, rods require "completed" 11cRAL chromophore to regenerate rhodopsin[16,17] and cannot use 11cROL. Because only 11cRAL can combine with an apo-opsin to form its cognate visual pigment, these observations suggest that cones contain an enzyme that oxidizes 11cROL to 11cRAL. In this work, we identified an 11cROL-dehydrogenase expressed in zebrafish cones. Using genetically modified zebrafish, we show that this enzyme is required for bleached cones to recover photosensitivity from 11cROL. Further, we show that the functional ortholog of ZCRDH in humans is RDH12, the only closely related protein that possesses 11cROL oxidase expressed in cone photoreceptors.

RESULTS

Screen for an 11cROL oxidase in cones

To begin our identification of the cone 11cROL oxidase, we looked for members of the short-chain dehydrogenase/reductase (SDR) family that are expressed in zebrafish cones. We began by searching a previously published single-cell RNA sequencing (scRNA-seq) dataset from normal adult zebrafish retinas[18] for mRNAs present in the cone cell clusters but reduced or absent from rod-cell clusters. These clusters included mRNAs for multiple known cone-specific proteins, such as M-cone opsin, G protein α-transducin 2, and cone arrestin. The set of cone-enriched zebrafish mRNAs also included two predicted protein products of the uncharacterized genes, zgc:153441 and si:dkey-23o4.6. Both exhibited features of the known retinol dehydrogenases (RDHs), including the catalytic tetrad and NAD(P)(H) cofactor-binding motif (GxxxGxG).[19] A genome duplication event occurred early in the teleost lineage, giving rise to paired ohnologs of many zebrafish genes.[20] At 68% identity, these predicted RDHs with cone-enriched expression were more similar to one another than to other proteins in the zebrafish database, suggesting that they are ohnologs. We provisionally named the protein encoded by zgc:153441 (GenBank: NP_001038920.1) "zebrafish cone RDH" (ZCRDH) and the presumptive ohnolog encoded by si:dkey-23o4.6 (GenBank: XP_021328703.1) "zebrafish cone RDH-like" (ZCRDH-L) (Figure S1).

Characterization of the *Zcrdh*-mutant zebrafish line

We acquired from Zebrafish International Resource Center (ZIRC), a zebrafish line with an A → G mutation in the highly conserved splice-acceptor site at the beginning of exon 6 within the *Zcrdh* gene. To define the effect of this mutation on the ZCRDH protein, we isolated mRNA from wild-type and *Zcrdh*-mutant zebrafish eyes and converted it to cDNA. We made primers for PCR from within exon 5 and the 3′ untranslated region of *Zcrdh*. The amplification product from *Zcrdh*-mutant zebrafish eyes was 15 nucleotides shorter than from wild-type zebrafish eyes. Sequence analysis showed that the protein product of the *Zcrdh*-mutant gene is missing five residues encoded by the 5′ end of exon 6. The deletion in ZCRDH resulting from the splice-site mutation is downstream of the N-terminal transmembrane α helix, the dinucleotide-binding site, and the catalytic tetrad motif[19] of ZCRDH.

To determine whether this deletion affected the stability of ZCRDH, we prepared a polyclonal Ab against a synthetic peptide (VLQLWDELKSNRLAKY) from near the N terminus of the predicted ZCRDH protein. This sequence is completely absent in ZCRDH-L, suggesting no cross reactivity of the anti-ZCRDH Ab with ZCRDH-L (Figure S2). We tested the Ab by immunoblotting protein homogenates from wild-type (AB strain) and *Zcrdh*-mutant zebrafish eyes and from HEK293T cells transfected with an expression plasmid containing the normal *Zcrdh* coding region. The antibody detected a protein band near the predicted size (37 kDa) in homogenates from wild-type zebrafish eyes. A faint band of the same size is visible in the lane containing homogenates from *Zcrdh*-mutant eyes (Figure 1A), suggesting that the deleted ZCRDH protein has substantially reduced stability. The slightly higher molecular mass of ZCRDH in HEK cell

Please cite this article in press as: Kaylor et al., RDH12 allows cone photoreceptors to regenerate opsin visual pigments from a chromophore precursor to escape competition with rods, Current Biology (2024), https://doi.org/10.1016/j.cub.2024.06.031

CellPress
OPEN ACCESS

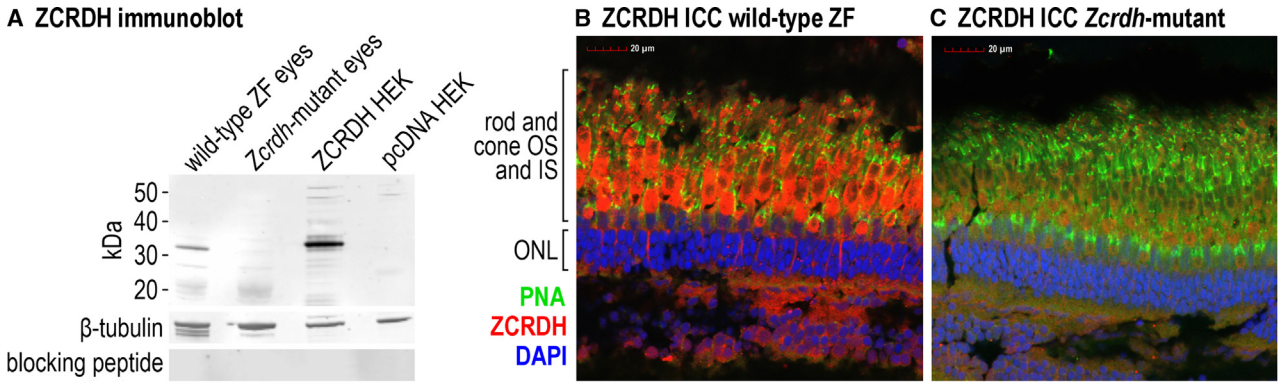

Figure 1. ZCRDH is expressed in zebrafish cone inner segments

An antibody was generated against an N-terminal peptide ZCRDH (product of the zgc:153441 gene) (Figure S2).

(A) The antibody was tested with four different protein homogenates: pcDNA3.1 HEK, HEK293T cells transfected with the non-recombinant expression plasmid, pcDNA3.1; ZCRDH HEK, HEK293T cells transfected with plasmid containing the ZCRDH coding region; wild-type ZF eyes, whole-eye tissues from wild-type (AB strain) zebrafish; and *Zcrdh*-mutant eyes, whole-eye tissues from *Zcrdh*-mutant zebrafish. The antibody detected a protein band of the predicted size (~37 kDa) in retinal homogenates from wild-type and ZCRDH-expressing HEK293T cells. The slightly higher molecular mass of ZCRDH in HEK-cell versus wild-type zebrafish retina homogenates is due to the presence of a FLAG epitope tag at the C terminus of recombinant ZCRDH. The same blot was re-probed with an antibody against β-tubulin as a protein loading control, shown below the ZCRDH immunoblot. A similar blot was probed with the ZCRDH antibody after preincubation with the immunizing peptide. Note the absence of signal in this control for Ab specificity.

(B) Immunohistochemistry performed on adult wild-type zebrafish retinal sections using ZCRDH Ab (red), peanut agglutinin (PNA) lectin to label the sheath surrounding cone outer segments (green), and the nuclear stain 4′,6-diamidino-2-phenylindole DAPI (blue). Scale bar, 20 μm. ZCRDH immunoreactivity is strongly present in cone inner segments.

(C) Immunocytochemistry performed on adult *Zcrdh*-mutant retinal sections using the same ZCRDH Ab, PNA, and DAPI labels as in (B). The region labeled "rod and cone IS and OS" corresponds to the region of rod and cone photoreceptor inner and outer segments, respectively. The region labeled "ONL" corresponds to the outer nuclear layer containing rod and cone photoreceptor nuclei. Scale bar, 20 μm. Note the greatly reduced labeling of cone inner segments in *Zcrdh*-mutant versus wild-type zebrafish retinas.

See also Figure S2.

versus wild-type zebrafish-eye homogenates (Figure 1A) is due to the presence of a FLAG epitope tag at the C terminus of recombinant ZCRDH.

We used the same anti-ZCRDH Ab for confocal immunocytochemistry of wild-type and *Zcrdh*-mutant zebrafish retina sections (Figures 1B and 1C). In addition, we reacted these retinal sections with DAPI to identify cell nuclei and peanut agglutinin (PNA) to label the matrix sheath surrounding cone OSs. ZCRDH immunoreactivity was strong in the inner segments of UV-, short-wavelength (S-), middle-wavelength (M-), and long-wavelength (L-) cones from wild-type zebrafish (Figure 1B). We also observed weak ZCRDH labeling of rod inner segments and no labeling of rod or cone OSs. The distribution of ZCRDH immunoreactivity in cone inner segments and RPE cells is consistent with the scRNA-seq data showing enriched expression of *Zcrdh* in cone and RPE cell clusters[18] (Figure S1). In contrast, immunocytochemistry with the same Ab on *Zcrdh*-mutant retina sections showed greatly reduced ZCRDH immunoreactivity with a similar cellular distribution. Together, the above observations suggest that the *Zcrdh* mutation is a severe hypomorph or a null.

Histology of wild-type and *Zcrdh*-mutant zebrafish retinas

To test for photoreceptor degeneration or other structural abnormalities in retinas due to the *Zcrdh* mutation, we performed histological analysis of retinal sections from 6-month-old wild-type and *Zcrdh*-mutant zebrafish. Total retina thickness was similar in fish of the two genotypes (Figures 2A and 2B). The number of rod and cone photoreceptor nuclei were also similar. We observed no significant differences in thickness of the OS layer, the outer nuclear layer (ONL), the inner nuclear layer (INL), the inner plexiform layer (IPL), or the ganglion cell layer (GCL) (Figures 2A and 2B). These findings suggest no photoreceptor degeneration or other morphological changes caused by the *Zcrdh* mutation in zebrafish up to 6 months of age.

Retinoid dynamics in the retinas of wild-type and *Zcrdh*-mutant zebrafish

To study the function of ZCRDH *in vivo*, we dark-adapted adult (5-month-old) wild-type (AB strain) and *Zcrdh*-mutant zebrafish overnight. We euthanized one group of both zebrafish lines, removed the eyes, prepared homogenates from the retinas and RPE, and extracted these homogenates for retinoid analysis by normal-phase high-performance liquid chromatography (HPLC). The remaining fish were exposed to 10 flashes from a strobe in a Ganzfeld integrating sphere that was estimated to bleach ~50% of visual pigments. Groups of fish from both lines were immediately euthanized, their eyes were collected, and individually homogenized for retinoid extraction and analysis. The remaining live fish were transferred to darkness. At 5, 30, and 60 min of post-bleach recovery in the dark, groups of fish from both lines were euthanized, their eyes collected, and homogenized for retinoid quantification. Data for 11cRAL, 11cROL, and 11-*cis*-retinyl palmitate (11cRP) are shown in Figures 3A–3C. Levels of 11cRAL were lower in *Zcrdh*-mutant versus wild-type retinas in the dark-adapted state and at 30 and 60 min post-bleach recovery (Figure 3A). This observation

Please cite this article in press as: Kaylor et al., RDH12 allows cone photoreceptors to regenerate opsin visual pigments from a chromophore precursor to escape competition with rods, Current Biology (2024), https://doi.org/10.1016/j.cub.2024.06.031

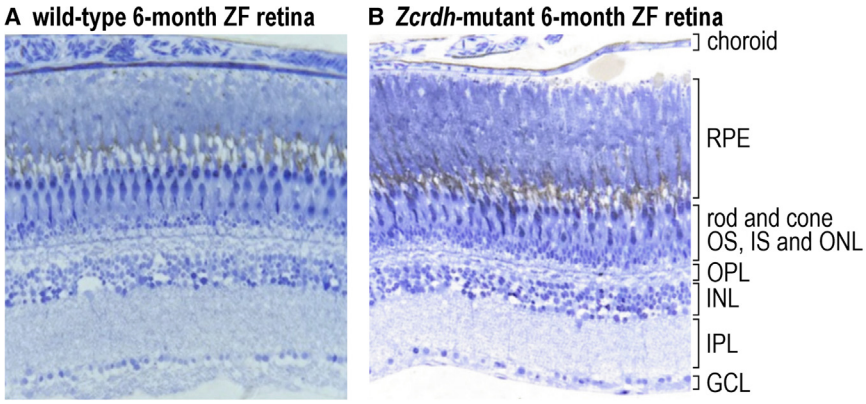

Figure 2. Histological analysis of retina sections from wild-type and *Zcrdh*-mutant zebrafish

Histologic sections from 6-month-old wild-type (A) and *Zcrdh*-mutant (B) zebrafish retinas. Sections were stained with 1% toluidine blue and 1% sodium borate and photographed with a 20× objective. Retina layers are identified to the right of (B). RPE, retinal pigment epithelium; rod and cone OS, IS, and ONL, rod and cone outer segments, inner segments, and outer nuclear layer (containing rod and cone photoreceptor nuclei); OPL, outer plexiform layer; INL, inner nuclear layer; IPL, inner plexiform layer; GCL, ganglion cell layer. Note the similar number of photoreceptor nuclei and similar thickness of retinal layers in wild-type and *Zcrdh*-mutant retinas.

suggests that loss of ZCRDH from zebrafish retinas causes reduced dark-adapted levels and delayed recovery of 11cRAL after a photobleach. Adult zebrafish retinas contain ~60% cones and ~40% rods. If we assume that loss of ZCRDH only affects chromophore regeneration in cones, the observed effect on total 11cRAL measured here reflects a nearly 2-fold underestimate of the actual effect on 11cRAL levels in *Zcrdh*-mutant cones. In contrast, levels of 11cROL were elevated in *Zcrdh*-mutant versus wild-type retinas in the dark-adapted state and early post-bleach (Figure 3B). We also observed dramatically higher levels of 11cRP, an insoluble storage form of 11cROL, in *Zcrdh*-mutant versus wild-type retinas under all conditions of light exposure (Figure 3C). Given that excess 11cROL is stored as 11cRP, levels of 11cRP are a useful surrogate for unused 11cROL. The observed higher levels of 11cROL and 11cRP in *Zcrdh*-mutant retinas suggests reduced utilization of 11cROL due to loss of 11cROL-oxidase activity in cone inner segments. These differences in retinoid dynamics between wild-type and *Zcrdh*-mutant eyes support the suggestion that ZCRDH functions as an 11cROL-oxidase in cone inner segments.

Microspectrophotometry

We used microspectrophotometry (MSP) of single, isolated photoreceptors to assess the capacity of wild-type and *Zcrdh*-mutant zebrafish cones to regenerate visual pigments from 11cROL. We adopted an approach similar to that used previously in tiger-salamander retina.[16,17] In brief, we isolated the retina and dispersed single cells onto coverslips in our recording chamber. We measured visible absorption spectra from individual M-cone, L-cone, and rod outer segments under four conditions: (1) dark-adapted, (2) after an ~90% photobleach, (3) after an ~90% photobleach followed by incubation with 15 μM 11cROL, and (4) after an ~90% photobleach followed by incubation with 15 μM 11cRAL (Figure 4). The top row (Figures 4A–4C) shows spectrophotometric data from wild-type (AB strain) zebrafish, whereas the bottom row (Figures 4D–4F) shows data from *Zcrdh*-mutant zebrafish. Following the photobleach, wild-type M and L cones regenerated their respective opsin pigments from added 11cROL (Figures 4A and 4B), whereas no rhodopsin regeneration from 11cROL was observed in bleached rods (Figure 4C). In *Zcrdh*-mutant retinas, however, no regeneration of opsin pigments was observed in photobleached M or L cones from added 11cROL (Figures 4D and 4E). Similar to wild-type rods, no regeneration of rhodopsin was observed in *Zcrdh*-mutant rods from 11cROL (Figure 4F). Instead, all *Zcrdh*-mutant photoreceptors remained bleached until the termination of the experiment. As a positive control, we incubated *Zcrdh*-mutant M cones, L cones, and rods with 11cRAL following the 90% photobleach. Here, we observed regeneration of all visual pigments to dark-adapted levels (Figures 4D–4F). These findings indicate that ZCRDH facilitates the conversion of 11cROL to 11cRAL for regeneration of opsin pigments in M and L cones. Loss of ZCRDH eliminates 11cROL-dependent regeneration of M-opsin and L-opsin in zebrafish cones, which defines the role of the cone 11cROL-oxidase.

Mammalian ortholog of ZCRDH

To identify the human ortholog of ZCRDH, we performed BLAST analysis using the amino acid sequence of zebrafish ZCRDH to probe the human protein database. The top seven human proteins most closely related to ZCRDH in order of increasing similarity were RDH10, RDH8, DHRS3, RDH14, RDH11, RDH13, and RDH12 (Table S1). Similarly, when we used ZCRDH-L to probe the human protein database, RDH12 was again the most similar at 56% amino acid identity. We performed a reciprocal BLAST search using human RDH12 to query the zebrafish protein database. The two most similar zebrafish proteins to human RDH12 are zebrafish RDH12 and RDH12-L, with ZCRDH at lower identity and similarity (Table S2). Three hypothetical zebrafish proteins, encoded by the genes si:dkey-73n8.3, si:dkey-94e7.2, and zgc:112332, were also detected in a BLAST search of the zebrafish protein database queried by human RDH12 (Table S2). We compared the dinucleotide-binding sites and catalytic tetrad motifs in the human proteins similar to ZCRDH and the zebrafish proteins similar to human RDH12. The dinucleotide-binding sites and catalytic tetrad motifs were absolutely conserved between zebrafish ZCRDH, human RDH11, RDH12, RDH13, and RDH14. Similarly, the dinucleotide-binding sites and catalytic tetrad motifs were absolutely conserved between human RDH12, zebrafish RDH12-L, zebrafish ZCRDH, and the three hypothetical zebrafish proteins similar to human RDH12. Identifying the mammalian ortholog of ZCRDH based on sequence comparisons is complicated by the presence of multiple, highly conserved SDR proteins in zebrafish and humans and by the large evolutionary distance (~400 Ma) that separates teleosts from mammals. Here, the similarity of orthologs arising

Please cite this article in press as: Kaylor et al., RDH12 allows cone photoreceptors to regenerate opsin visual pigments from a chromophore precursor to escape competition with rods, Current Biology (2024), https://doi.org/10.1016/j.cub.2024.06.031

CellPress
OPEN ACCESS

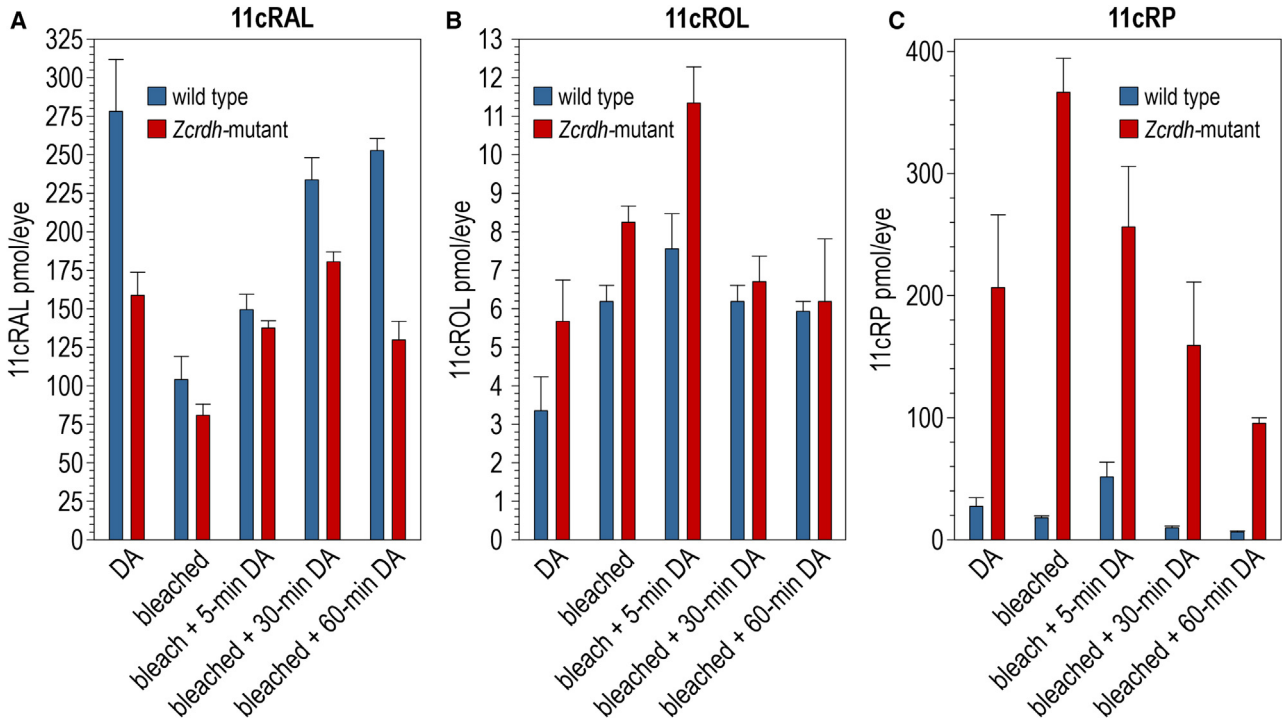

Figure 3. Retinoid profiles of *Zcrdh*-mutant and wild-type zebrafish eyes under different light-exposure conditions

Whole-eye retinoid profiles of age-matched *Zcrdh*-mutant (red) and AB wild-type (blue) adult zebrafish (5 months old) under different light-exposure conditions: DA, overnight dark-adapted; bleached, immediately following an ~50% photobleach; bleach + 5, 30, or 60 min DA, bleached followed by the indicated period of recovery in the dark.

(A) 11cRAL chromophore levels in the eyes of wild-type or *Zcrdh*-mutant zebrafish after indicated light exposures.

(B) 11cROL levels in the eyes of wild-type or *Zcrdh*-mutant zebrafish after indicated light exposures.

(C) 11cRP levels in the eyes of wild-type or *Zcrdh*-mutant zebrafish after indicated light exposures. Error bars show standard deviation of the mean for four replicates (n = 4).

through speciation is obscured by the greater similarity of paralogs that arose through gene duplication. Sequence analysis suggests four candidates for the mammalian ortholog of ZCRDH in order of similarity: RDH12, RDH13, RDH11, and RDH14 (Table S1).

Expression of mRNAs related to ZCRDH in zebrafish and mammalian retinas

An absolute requirement of the cone 11cROL oxidase is that it be expressed in cones. Accordingly, we analyzed the expression of human *Rdh12*-paralogous mRNAs in zebrafish retinas by scRNA-seq analysis.[18] In zebrafish retinas, the *Zcrdh* and *Zcrdh-L* mRNAs are both expressed predominantly in cone cell clusters, with an additional expression of *Zcrdh* in RPE cells (Figure S1). Importantly, neither *Rdh12*, *Rdh12-L*, nor mRNAs for the three hypothetical zebrafish proteins similar to human RDH12 (*si:dkey-73n8.3*, *si:dkey-94e7.2*, and *zgc:112332*) showed significant expression in cones (Figure S1). We also analyzed the expression of *Zcrdh* paralogs in human retinas by scRNA-seq analysis.[21] In human retinas, the *Rdh12* and *Rdh8* mRNAs were abundantly expressed in cone and rod-cell clusters, whereas the *Rdh10*, *Rdh11*, *Rdh13*, *Rdh14*, and *Dhrxs* mRNAs were present at reduced levels in cones and rods (Figure S3). The presence of RDH8 in rods and cones makes sense because this protein is responsible for reduction of atRAL released from bleached visual pigments in rod and cone OSs.[22] Because RDH8 is not present in rod or cone inner segments, it is unlikely to serve as the mammalian cone 11cROL oxidase. These scRNA-seq results are most consistent with RDH12 serving as the mammalian cone 11cROL oxidase but do not rule out the remaining human RDH candidates.

11cROL-oxidase activity of ZCRDH and related mammalian proteins

Because the utilization of 11cROL to regenerate cone visual pigments requires 11cROL-oxidase activity, we transfected plasmids containing the coding regions of mammalian RDH11, RDH12, RDH13, RDH14, or zebrafish ZCRDH into HEK293T cells. Homogenates from these cells were used as enzyme sources in assays to measure nicotinamide adenine dinucleotide phosphate $(NADP)^+$-dependent conversion of 11cROL to 11cRAL. Similar rates of 11cRAL formation were observed with cell homogenates containing ZCRDH and RDH12, whereas no 11cRAL was produced by homogenates containing RDH11, RDH13, or RDH14 or non-recombinant pcDNA3.1 (Figure 5A). Additionally, we transfected plasmids containing the coding regions for zebrafish ZCRDH-L, RDH12, and RDH12-L, plus carp ZCRDH and RDH13-L into HEK293T cells. Homogenates from these cells were likewise used as enzyme sources in assays to measure conversion of 11cROL to 11cRAL. Zebrafish

Please cite this article in press as: Kaylor et al., RDH12 allows cone photoreceptors to regenerate opsin visual pigments from a chromophore precursor to escape competition with rods, Current Biology (2024), https://doi.org/10.1016/j.cub.2024.06.031

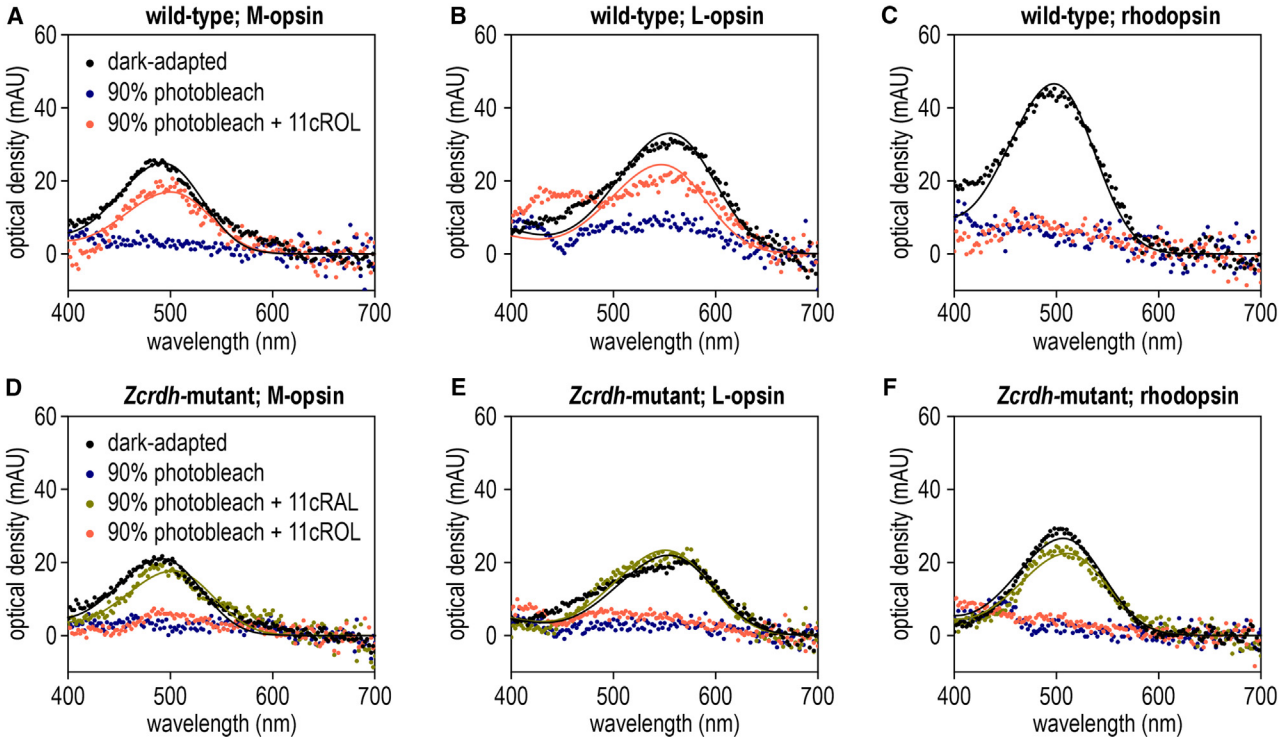

Figure 4. Absent regeneration of cone visual pigments in *Zcrdh*-mutant retinal explants following a photobleach and treatment with 11cROL chromophore precursor

Absorbance spectra of wild-type and *Zcrdh*-mutant zebrafish photoreceptors.

(A) Average absorbance spectra from wild-type zebrafish M cones. The mean peak optical densities (± SEM) were OD_{DA} = 0.024 ± 0.0025, OD_{bleach} = 0.0036 ± 0.0033, and OD_{11cROL} = 0.018 ± 0.0043.

(B) Average absorbance spectra from wild-type zebrafish L cones. The mean peak optical densities were OD_{DA} = 0.030 ± 0.0043, OD_{bleach} = 0.0091 ± 0.0041, and OD_{11cROL} = 0.021 ± 0.0039.

(C) Average absorbance spectra from wild-type zebrafish rods. The mean peak optical densities were OD_{DA} = 0.044 ± 0.0050, OD_{bleach} = 0.0076 ± 0.0031, and OD_{11cROL} = 0.0060 ± 0.0019.

(D) Average absorbance spectra from *Zcrdh*-mutant zebrafish M cones. The mean peak optical densities were OD_{DA} = 0.021 ± 0.0040, OD_{bleach} = 0.0023 ± 0.0099, OD_{11cROL} = 0.0059 ± 0.0038, and OD_{11cRAL} = 0.017 ± 0.0028.

(E) Average absorbance spectra from *Zcrdh*-mutant zebrafish L cones. The mean peak optical densities were OD_{DA} = 0.018 ± 0.0037, OD_{bleach} = 0.0033 ± 0.0070, OD_{11cROL} = 0.0052 ± 0.0035, and OD_{11cRAL} = 0.021 ± 0.0017.

(F) Average absorbance spectra from *Zcrdh*-mutant zebrafish rods. The mean peak optical densities were OD_{DA} = 0.029 ± 0.0028, OD_{bleach} = 0.0020 ± 0.0028, OD_{11cROL} = 0.0050 ± 0.0024, and OD_{11cRAL} = 0.023 ± 0.0020. Data from dark-adapted and regenerated cells are fitted with A1 nomograms with the following parameters: WT DA M-cone, λ_{max} = 492 nm, OD_{peak} = 0.025; WT 11cROL M-cone, λ_{max} = 500 nm, OD_{peak} = 0.017; WT DA L-cone, λ_{max} = 555 nm, OD_{peak} = 0.033; WT 11cROL L-cone, λ_{max} = 547 nm, OD_{peak} = 0.024; WT DA rod, λ_{max} = 498 nm, OD_{peak} = 0.047; *Zcrdh*-mutant DA M-cone, λ_{max} = 502 nm, OD_{peak} = 0.018; *Zcrdh*-mutant 11cRAL M-cone, λ_{max} = 491 nm, OD_{peak} = 0.021; *Zcrdh*-mutant DA L-cone, λ_{max} = 554 nm, OD_{peak} = 0.022; *Zcrdh*-mutant 11cRAL L-cone, λ_{max} = 551 nm, OD_{peak} = 0.023; *Zcrdh*-mutant DA rod, λ_{max} = 507 nm, OD_{peak} = 0.027; *Zcrdh*-mutant 11cRAL rod, λ_{max} = 510 nm, OD_{peak} = 0.022.

ZCRDH-L and carp ZCRDH possessed high 11cROL oxidase activities (Figure 5B), similar to zebrafish ZCRDH and human RDH12 (Figure 5A). Importantly, zebrafish RDH12 and RDH12-L exhibited no 11cROL-oxidase activities (Figure 5B). The coding region for each enzyme included a C-terminal FLAG epitope tag, which allowed us to compare directly levels of each expressed protein in the homogenates. Immunoblot analysis of these homogenates with an anti-FLAG antibody showed similar levels of each enzyme protein in the assay mixtures (Figure 5C). Accordingly, the absence of 11cROL-oxidase activity in HEK homogenates expressing human RDH11, RDH13, and RDH14 plus zebrafish RDH12 and RDH12-L is not due to low expression of these proteins in HEK cells but instead because of their very low intrinsic 11cROL-oxidase activities. These results exclude human RDH11, RDH13, and RDH14 as candidates for the cone 11cROL oxidase and suggest that RDH12 is the functional ortholog in mammals of zebrafish ZCRDH. Interestingly, zebrafish RDH12 and RDH12-L, despite their similarity to human RDH12 (Table S2), exhibited no 11cROL-oxidase activity.

11cROL-oxidase kinetics of ZCRDH and RDH12

To corroborate further the functional similarity of ZCRDH and human RDH12, we performed Michaelis-Menton analysis of ZCRDH and RDH12 in the relevant 11cROL-oxidase direction. Here, again, the activities were remarkably similar, with K_Ms of 0.78 and 0.69 μM 11cROL, respectively (Figures 5D and 5E). Moreover, because the levels of ZCRDH and RDH12 protein were comparable in HEK293T cells (Figure 5C), the V_{max} values can be meaningfully compared at 16.1 and 13.1 pmol/mg/min, respectively (Figures 5D and 5E). The close agreement between

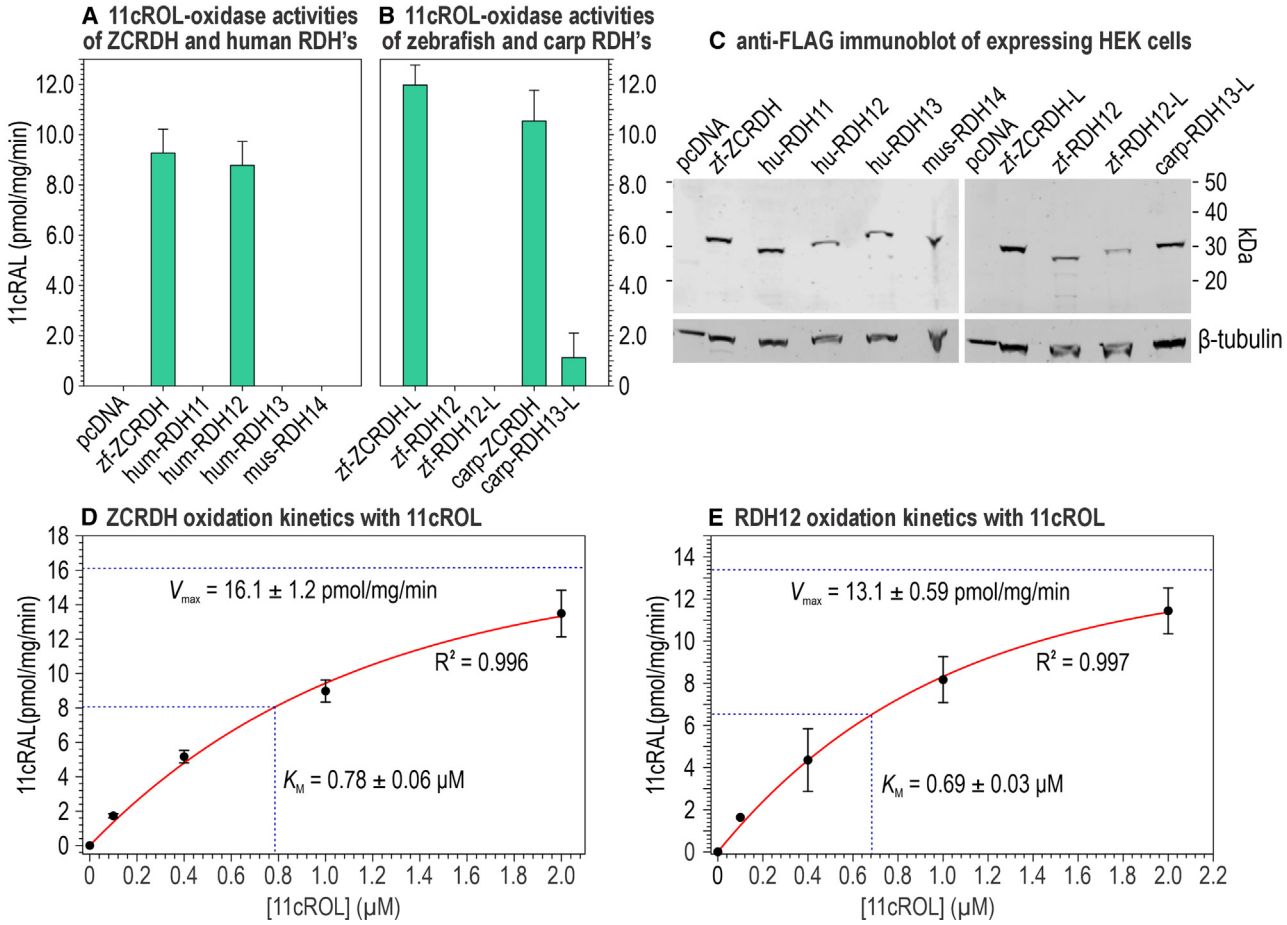

Figure 5. 11cROL-oxidase activity of ZCRDH and various mammalian RDH candidates for the cone 11cROL-oxidase and substrate kinetics for ZCRDH and RDH12

HEK293T cells were transfected with non-recombinant pcDNA3.1 or the same plasmid containing the coding regions for the indicated proteins. All clones were made with a C-terminal FLAG tag. Assays were carried out using homogenate of the transfected cells as an enzyme source with 2 μM 11cROL and 1 mM $NADP^+$ cofactor for 1 min at 37°C with gentle agitation.

(A) 11cROL-oxidase activities (11cRAL synthesis): zf-ZCRDH, zebrafish ZCRDH; hum-RDH11, human RDH11; hum RDH12, human RDH12; hum-RDH13, human RDH13; and mus-RDH14, mouse RDH14.

(B) 11cROL-oxidase activities: zf-ZCRDH-L, zebrafish ZCRDH-like; zf-RDH12, predicted zebrafish RDH12; zf-RDH12-L, predicted zebrafish RDH12-like; carp ZCRDH, carp ZCRDH; and carp RDH13-L, carp RDH13-like.

(C) Immunoblots containing equal protein amounts of HEK293T cell homogenates transfected with the indicated plasmids and reacted with an anti-FLAG antibody. Note the similar intensities of immunoreactive bands containing the different proteins. The same blot was re-probed with an antibody against β-tubulin as a protein loading control, shown below the anti-FLAG immunoblot.

(D and E) (D) Michaelis-Menton analysis of 11cROL oxidation of ZCRDH and (E) human RDH12 using the indicated 11cROL concentrations and 1 mM $NADP^+$. The assay conditions for kinetic analysis are as described in this figure. Calculated K_M and V_{max} values are shown. Error bars show standard deviation of the mean for three replicates (n = 3).

See also Figures S1 and S3 and Tables S1 and S2.

these kinetic parameters is further evidence that ZCRDH and RDH12 are functionally orthologous 11cROL oxidases.

Redox-coupled 11cROL oxidation and atRAL reduction of ZCRDH and RDH12

Several years ago, Sato et al. described an enzyme activity in cone inner segments of carp that catalyzes the simultaneous oxidation of 11cROL to 11cRAL and reduction of atRAL to atROL.[23] The carp protein responsible for this activity was tentatively identified as RDH13-L, which is orthologous to RDH14 in mammals.[24] We acquired cDNAs for carp ZCRDH and RDH13-L, which we expressed in HEK293T cells. We assayed homogenates of these cells for 11cROL-oxidase activities. Carp ZCRDH exhibited high 11cROL-oxidase activity (Figure 5B), similar to zebrafish ZCRDH and human RDH12 (Figure 5A), whereas carp RDH13-L had lower activity (Figure 5B), and mouse RDH14 had no detectable activity (Figure 5A). These findings rule against RDH14 as the cone 11cROL oxidase in mammals.

To test for redox coupling, we prepared homogenates of HEK293T cells transfected with plasmids containing the zebrafish ZCRDH or the human RDH12 cDNAs. These were used as

Please cite this article in press as: Kaylor et al., RDH12 allows cone photoreceptors to regenerate opsin visual pigments from a chromophore precursor to escape competition with rods, Current Biology (2024), https://doi.org/10.1016/j.cub.2024.06.031

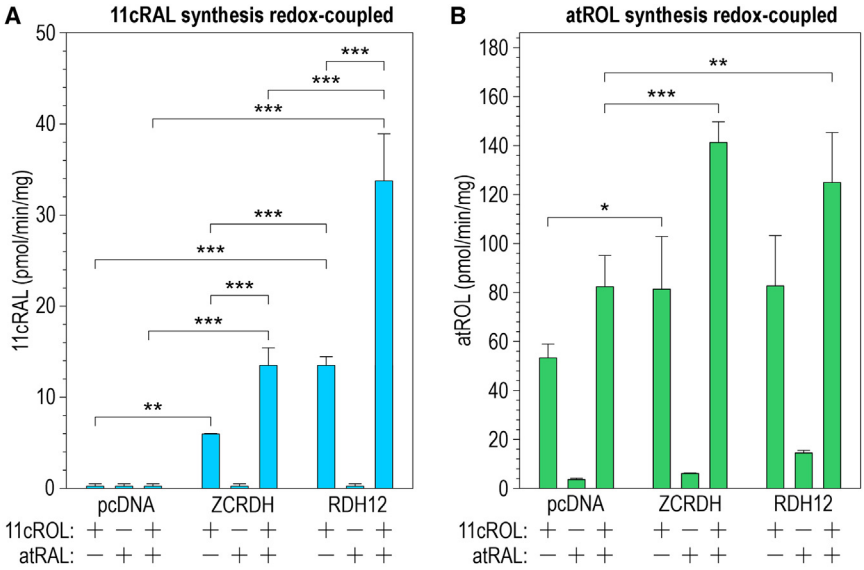

Figure 6. Comparison of redox-coupled catalytic activities of ZCRDH and human RDH12

(A) 11cRAL synthesis by ZCRDH and human RDH12 in enzyme assays containing 5 μM of the indicated substrate(s) and no added dinucleotide cofactor.

(B) atROL synthesis by ZCRDH and human RDH12 containing 5 μM of the indicated substrate(s) and no added NADP(H) cofactor. Error bars at each concentration show standard deviation of the mean for three replicates ($n = 3$).

Datasets were analyzed by one-way ANOVA followed by Student-Newman-Keuls t test to test for significance between different test groups. $^{*}p \leq 0.05$; $^{**}p \leq 0.01$; $^{***}p \leq 0.001$. Test group comparisons without indicated p values are not significant ($p > 0.05$).

enzyme sources in reactions containing 11cROL, atRAL, or both, all without added NADP(H). No 11cRAL synthesis was observed in negative-control (non-recombinant pcDNA) reactions containing 11cROL, atRAL, or both (Figure 6A). This observation suggests that HEK293T cells possess no intrinsic 11cROL-oxidase activity. Reactions containing ZCRDH or RDH12 showed 11cRAL synthesis when 11cROL was present in the mixtures, but not when atRAL was present alone. Importantly, we observed increased 11cRAL synthesis with ZCRDH or RDH12 in reactions containing both 11cROL and atRAL versus reactions containing 11cROL alone (Figure 6A). This observation shows that both ZCRDH and RDH12 carry out coupled oxidation of 11cROL and reduction of atRAL. In the control reactions containing non-recombinant plasmid, we observed atROL synthesis in the presence of 11cROL or 11cROL plus atRAL, with little atROL synthesis in reactions containing only atRAL (Figure 6B). This was probably caused by thermal isomerization of 11cROL to atROL. The increased synthesis of atROL in the presence of 11cROL and atRAL versus 11cROL alone may reflect additional reduction of atRAL to atROL through redox coupling. This observation suggests further that HEK293T cells possess an intrinsic atRAL-reductase activity. When ZCRDH- or RDH12-containing homogenates were added to the reaction mixtures, we observed modestly increased atROL production versus similar reactions without added enzyme. These observations are consistent with ZCRDH and RDH12 performing coupled oxidation of 11cROL and reduction of atRAL beyond the background thermal isomerization of 11cROL to atROL. Subtracting background synthesis of atROL in negative-control reactions containing only pcDNA3.1 plus 11cROL and atRAL substrates (Figure 6B), we observed similar production of 11cRAL (Figure 6A) and atROL (Figure 6B) at ~34 and ~40 pmol/min/mg, respectively, generally consistent with equimolar reaction products predicted in a redox-coupled reaction. These results also suggest that other retinol oxidoreductases besides RDH13-L,[24] ZCRDH, and RDH12 (Figures 6A and 6B) may display increased turnover in the presence of both oxidizing and reducing substrates without added NADP(H) cofactor.

DISCUSSION

The goal of this study was to identify the protein that allows cones, but not rods, to regenerate their photobleached visual pigments using 11cROL released by Müller cells. Our detection of ZCRDH as this protein is based on the corroboration of several predictions: (1) the cone 11cROL dehydrogenase should exhibit cone-enriched expression. The *Zcrdh* mRNA showed enriched expression in cone- versus rod-cell clusters by scRNA-seq analysis[18] (Figure S1). By immunocytochemistry, ZCRDH was abundantly present in cone inner segments and present at lower abundance in rod inner segments (Figures 1B and 1C). (2) Loss of the cone 11cROL oxidase from mutant zebrafish retinas should result in decreased 11cRAL, increased 11cROL, and increased 11cRP due to reduced utilization of 11cROL for chromophore synthesis. These are the findings that we observed in wild-type versus *Zcrdh*-mutant retinas during a retinoid dynamics experiment involving a photobleach and recovery in the dark (Figure 3). (3) Loss of the cone 11cROL oxidase from mutant zebrafish retinas should abolish the capacity of cones to regenerate visual pigments from added 11cROL following a photobleach. The capacity of cones to regenerate visual pigments from added 11cRAL should not be affected. We performed MSP analysis on isolated M cones, L cones, and rods from wild-type and *Zcrdh*-mutant retinas. The findings from this experiment were exactly as predicted (Figure 4). (4) The candidate protein should exhibit 11cROL-oxidase activity. We performed enzyme assays on zebrafish ZCRDH, human RDH11, human RDH12, human RDH13, or mouse RDH14 to measure 11cROL-oxidase activity. ZCRDH and RDH12 showed robust production of 11cRAL, whereas the other proteins in this group showed no 11cROL-oxidase activity (Figure 5A). Together, these observations establish that ZCRDH is the cone 11cROL dehydrogenase in zebrafish that allows cones, but not rods, to regenerate their opsin visual pigments from exogenous 11cROL after a photobleach.

We identified RDH12 as the mammalian counterpart of ZCRDH based on several observations. First, the primary

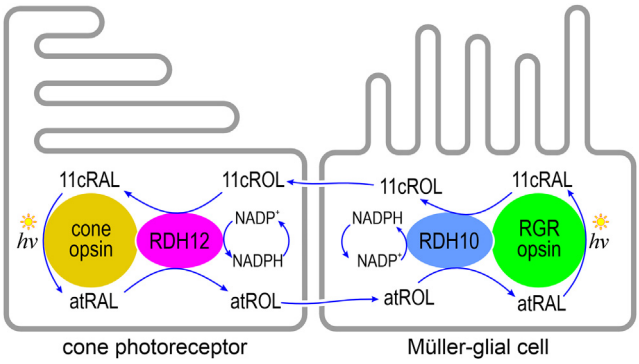

Figure 7. Proposed model for the photic cone visual cycle in Müller glial cells and cone photoreceptors

Absorption of a photon (*hv*) by a cone-opsin pigment isomerizes the 11cRAL to atRAL, activating visual transduction. Shortly afterward, atRAL dissociates from the opsin, is reduced to atROL by RDH12, and is released into the extracellular space for recycling. The atROL is taken up by the Müller cell where it is re-oxidized by RDH10 to atRAL, which binds covalently to apo-RGR opsin. Absorption of a photon by RGR opsin isomerizes atRAL to 11cRAL.[30] The 11cRAL is reduced, again by RDH10, to 11cROL, which is released by Müller cells into the extracellular space.[15] Finally, the 11cROL is taken up by the cone photoreceptor where it is oxidized by RDH12 to 11cRAL, which combines with cone apo-opsin to form a new cone visual pigment. Because only cones can utilize 11cROL to regenerate their visual pigments, the visual cycle in Müller cells helps cones avoid competition with rods for chromophore under bright-light conditions.

sequence of human RDH12 is most similar to that of ZCRDH (Table S1). In common with ZCRDH (Figure 1B), RDH12 is abundantly present in cone inner segments.[25] A role for mammalian RDH12 as an 11cROL oxidase that provides 11cRAL to cones was proposed by Haeseleer et al.[8] Importantly, RDH12 is the only candidate protein possessing 11cROL-oxidase activity (Figure 5A). In contrast, the other candidate proteins, RDH11, RDH13, and RDH14, possessed no 11cROL oxidase activity (Figure 5A). Further, the kinetic parameters, V_{max} and K_M, for 11cROL-oxidase activity were remarkably similar for ZCRDH and human RDH12 (Figures 5D and 5E) expressed at similar levels in HEK293T cells (Figure 5C).

The presence of ZCRDH and RDH12 in the inner segments of both rods and cones raises the question of how cones, but not rods, are able to regenerate visual pigments from 11cROL. Following photoactivation, the much higher rates of visual-pigment decay (release of atRAL) and reduction of atRAL to atROL in cones versus rods provides a clue. For example, the time constant for decay of salamander red-cone opsin is 70-fold faster than for decay of rhodopsin, whereas the time constant for atRAL reduction in red cones is 38-fold faster than in rods.[26] Two enzymes catalyze reduction of atRAL to atROL in photoreceptors: RDH8 is in the OSs of rods and cones,[22] whereas RDH12 is in the inner segments.[25] In rods, the preponderance of atRAL produced by photobleaching of rhodopsin is reduced in OSs by RDH8, whereas in cones, atRAL produced by photobleaching of cone opsins takes place in both inner and OSs by RDH8 and RDH12, respectively.[27] $NADP^+$, the oxidizing cofactor used by RDH12 to convert 11cROL to 11cRAL (Figure 5A), is generated from NADPH through reduction of atRAL. In accordance with the above observations, $NADP^+$ is produced at much higher rates in cone versus rod inner segments during light exposure. Most cells contain a large excess of NADPH over $NADP^+$; hence, the availability of $NADP^+$ is rate limiting. The greater availability of $NADP^+$ in cone versus rod inner segments may explain why cones, but not rods, are able to regenerate their visual pigments from 11cROL when the inner segments of both cell types express RDH12. Further, the redox-coupling mechanism discussed above would not permit RDH12 in rod inner segments to oxidize significant 11cROL, because atRAL produced following photoactivation of rhodopsin is mainly reduced to atROL by RDH8 in OSs and hence is unavailable to serve as an electron acceptor for 11cROL oxidation by RDH12 in rods.

Our model for the cone visual cycle is shown in Figure 7. Absorption of a photon by an opsin visual pigment in a cone OS isomerizes the 11cRAL chromophore to atRAL, activating the pigment and hence visual transduction. Shortly afterward, the pigment decays to yield free atRAL and apo-opsin, which is insensitive to light. The atRAL is reduced by ZCRDH/RDH12 to atROL, which is released into the confined extracellular space defined by the cone inner segment and Müller cell apical processes.[28,29] Within Müller cells, the atROL is oxidized by RDH10 to atRAL, which combines with apo-RGR-opsin to form holo-RGR in Müller-cell internal membranes.[9] In contrast to the visual opsins in photoreceptors, RGR opsin covalently binds atRAL in the dark, which it isomerizes to 11cRAL upon absorption of a photon[30] and subsequently dissociates, releasing free 11cRAL.[31] RGR opsin was shown to pair functionally with RDH10 to affect the multi-step, light-dependent conversion of atROL to 11cROL.[15] This activity was observed in cultured HEK293T cells expressing both RGR opsin and RDH10 and in retinal fractions from normal but not *Rgr*−/− mutant mice.[15] The 11cROL is released into the extracellular space between Müller cells and cone inner segments. Finally, the 11cROL is taken up into the cone inner segment where it is oxidized by RDH12 to 11cRAL, which combines with cone apo-opsin to form a new cone-opsin visual pigment. Photic synthesis of chromophore for cone visual pigments offers important advantages over thermal regeneration of rhodopsin by the canonical visual cycle in RPE cells. With photic regeneration, the rate of chromophore synthesis scales directly with light intensity, whereas metabolic regeneration is limited by the slow turnover rate of Rpe65.[1] Also, photic regeneration uses light as an energy source, whereas metabolic regeneration involves consumption of an activated fatty acid (+7.5 kcal/mol) for each photon absorbed. Another feature of the cone visual cycle is that it involves two simultaneous redox reactions of retinol and retinaldehyde, each carried out by a single enzyme; RDH12 affects reduction of atRAL and oxidation of 11cROL in cone inner segments, whereas RDH10 affects oxidation of atROL and reduction of 11cRAL in Müller cells (Figure 7). These paired reactions provide self-renewing supplies of dinucleotide cofactor in cone inner segments and Müller cells, further avoiding the need for input of metabolic energy to synthesize NADPH. Instead, the six reactions of this pathway are powered by light through "forward" photoisomerization of cone opsin and "reverse" photoisomerization of RGR opsin.

How do cones benefit from the capacity to regenerate their visual pigments from 11cROL? The retinas of many mammals

contain a large preponderance of rods over cones (~20:1 in humans). Further, the rod photoresponse saturates when exposed to moderately bright light (~1,000 rhodopsin photoisomerizations per second[32]) with little recovery even after long light exposures,[33] whereas cones remain responsive to bright light under background illumination causing greater than 10^6 photoisomerizations per second.[34,35] Importantly, saturated rods continue churning through chromophore in bright light despite contributing nothing to useful vision. Hence, in a daylight-illuminated retina, cones face arduous competition from rods for the limited supply of chromophore. By taking up 11cROL and converting it "in-house" to 11cRAL, cones escape competition from rods. In fact, this arrangement obliges rods to help regenerate cone visual pigments, because atROL released by photobleached rods is taken up by Müller cells, in addition to RPE cells, and converted to 11cROL for uptake by cones, but not rods. The cone visual cycle can thus be understood as a "private pipeline" of chromophore precursor to cones. The capacity of cone photoreceptors to regenerate their photobleached visual pigments using 11cROL is likely critical to the ability of humans and other diurnal vertebrates to maintain continuous vision during daylight.

Mutations in the human *Rdh12* gene cause a rapidly progressive retinal dystrophy called Leber congenital amaurosis (LCA), which begins during infancy and leads to severe visual loss by adulthood.[36] LCA accounts for 5% of all inherited retinal dystrophies and is responsible for 20% of legal blindness in children. Approximately 10% of LCA cases are caused by mutations in *Rdh12*. *Rdh12*-mediated LCA was thought to result from loss of RDH12-reductase activity, which eliminates retinaldehyde and other toxic aldehydes from photoreceptor inner segments.[37] However, patients with LCA caused by *Rdh12* mutations were found to exhibit severe central-retinal abnormalities with relative sparing of rod function.[38] Further, LCA-associated mutations in *Rdh12* cause decreased 11cRAL synthesis due to disruption of the visual cycle.[39] As shown here, loss of ZCRDH in mutant zebrafish retinas also resulted in decreased synthesis of 11cRAL-chromophore (Figure 3A). Together, these results suggest that loss of the 11cROL-oxidase activity in cones plays a role in the etiology of *Rdh12*-mediated LCA. Our finding that RDH12 is the likely cone 11cROL-oxidase in humans may lead to new understanding into the cause of this severe retinal dystrophy of children.

STAR★METHODS

Detailed methods are provided in the online version of this paper and include the following:

SUPPLEMENTAL INFORMATION

Supplemental information can be found online at https://doi.org/10.1016/j.cub.2024.06.031.

ACKNOWLEDGMENTS

This work was supported by NEI, National Institutes of Health grants R01-EY024379 (G.H.T.), R01 EY001844 (G.L.F.), R01 EY029817 (A.P.S.), and Core Grant P30 EY00331 to the Jules Stein Eye Institute. Additional funding includes a Research to Prevent Blindness Stein Innovation Award (G.H.T.) and a Research to Prevent Blindness unrestricted grant to the Jules Stein Eye Institute. G.H.T. is the Charles Kenneth Feldman Professor of Ophthalmology at UCLA. We would like to thank Jane Hu and Yuekan Jiao for their expert training and guidance in immunohistochemistry and histology. We would also like to thank Linda Dong for her expert training and support in zebrafish care.

AUTHOR CONTRIBUTIONS

G.H.T. conceived the project. G.H.T., A.P.S., G.L.F., R.F., and J.J.K. designed the experimental procedures. J.J.K., R.F., C.K.B., M.H., D.S.-W., T.H., T.N., and V.M. performed and optimized the experiments. J.J.K. and R.F. analyzed the data. J.J.K. identified the protein from published scRNA-seq datasets. J.J.K. performed histology and immunohistochemistry with the assistance of M.H., T.N., and V.M. J.J.K. performed retinoid profiling of zebrafish with the assistance of C.K.B. and T.H. Western blot analysis was performed by D.S.-W. Microspectrophotometry was performed by R.F. Enzyme activity and kinetic assays were performed by D.S.-W. and T.H. G.H.T. wrote the paper with contributions from J.J.K., A.P.S., and G.L.F. Funding acquisition, G.H.T, A.P.S., and G.L.F.

DECLARATION OF INTERESTS

The authors declare no competing interests.

Received: January 20, 2024
Revised: May 11, 2024
Accepted: June 10, 2024
Published: July 8, 2024

REFERENCES

1. Mata, N.L., Radu, R.A., Clemmons, R.C., and Travis, G.H. (2002). Isomerization and oxidation of vitamin a in cone-dominant retinas: a novel pathway for visual-pigment regeneration in daylight. Neuron *36*, 69–80. https://doi.org/10.1016/s0896-6273(02)00912-1.
2. Goldstein, E.B. (1970). Cone pigment regeneration in the isolated frog retina. Vision Res. *10*, 1065–1068. https://doi.org/10.1016/0042-6989(70)90082-9.
3. Hood, D.C., and Hock, P.A. (1973). Recovery of cone receptor activity in the frog's isolated retina. Vision Res. *13*, 1943–1951. https://doi.org/10.1016/0042-6989(73)90065-5.
4. Wang, J.S., and Kefalov, V.J. (2009). An alternative pathway mediates the mouse and human cone visual cycle. Curr. Biol. *19*, 1665–1669. https://doi.org/10.1016/j.cub.2009.07.054.
5. Bunt-Milam, A.H., and Saari, J.C. (1983). Immunocytochemical localization of two retinoid-binding proteins in vertebrate retina. J. Cell Biol. *97*, 703–712. https://doi.org/10.1083/jcb.97.3.703.

6. Huang, J., Possin, D.E., and Saari, J.C. (2009). Localizations of visual cycle components in retinal pigment epithelium. Mol. Vis. *15*, 223–234.
7. Wu, B.X., Moiseyev, G., Chen, Y., Rohrer, B., Crouch, R.K., and Ma, J.X. (2004). Identification of RDH10, an all-trans retinol dehydrogenase, in retinal Muller cells. Invest. Ophthalmol. Vis. Sci. *45*, 3857–3862. https://doi.org/10.1167/iovs.03-1302.
8. Haeseleer, F., Jang, G.F., Imanishi, Y., Driessen, C.A.G.G., Matsumura, M., Nelson, P.S., and Palczewski, K. (2002). Dual-substrate specificity short chain retinol dehydrogenases from the vertebrate retina. J. Biol. Chem. *277*, 45537–45546. https://doi.org/10.1074/jbc.M208882200.
9. Pandey, S., Blanks, J.C., Spee, C., Jiang, M., and Fong, H.K. (1994). Cytoplasmic retinal localization of an evolutionary homolog of the visual pigments. Exp. Eye Res. *58*, 605–613. https://doi.org/10.1006/exer.1994.1055.
10. Das, S.R., Bhardwaj, N., Kjeldbye, H., and Gouras, P. (1992). Muller cells of chicken retina synthesize 11-cis-retinol. Biochem. J. *285*, 907–913. https://doi.org/10.1042/bj2850907.
11. Jablonski, M.M., and Iannaccone, A. (2000). Targeted disruption of Muller cell metabolism induces photoreceptor dysmorphogenesis. Glia *32*, 192–204. https://doi.org/10.1002/1098-1136(200011)32:2<192::aid-glia80>3.0.co;2-6.
12. Mata, N.L., Ruiz, A., Radu, R.A., Bui, T.V., and Travis, G.H. (2005). Chicken retinas contain a retinoid isomerase activity that catalyzes the direct conversion of all-trans-retinol to 11-cis-retinol. Biochemistry *44*, 11715–11721. https://doi.org/10.1021/bi050942m.
13. Peng, Y.R., Shekhar, K., Yan, W., Herrmann, D., Sappington, A., Bryman, G.S., van Zyl, T., Do, M.T.H., Regev, A., and Sanes, J.R. (2019). Molecular classification and comparative taxonomics of foveal and peripheral cells in primate retina. Cell *176*, 1222–1237.e22. https://doi.org/10.1016/j.cell.2019.01.004.
14. Betts-Obregon, B.S., Gonzalez-Fernandez, F., and Tsin, A.T. (2014). Interphotoreceptor retinoid-binding protein (IRBP) promotes retinol uptake and release by rat Muller cells (rMC-1) in vitro: implications for the cone visual cycle. Invest. Ophthalmol. Vis. Sci. *55*, 6265–6271. https://doi.org/10.1167/iovs.14-14721.
15. Morshedian, A., Kaylor, J.J., Ng, S.Y., Tsan, A., Frederiksen, R., Xu, T., Yuan, L., Sampath, A.P., Radu, R.A., Fain, G.L., et al. (2019). Light-driven regeneration of cone visual pigments through a mechanism involving RGR opsin in Muller glial cells. Neuron *102*, 1172–1183.e5. https://doi.org/10.1016/j.neuron.2019.04.004.
16. Jones, G.J., Crouch, R.K., Wiggert, B., Cornwall, M.C., and Chader, G.J. (1989). Retinoid requirements for recovery of sensitivity after visual-pigment bleaching in isolated photoreceptors. Proc. Natl. Acad. Sci. USA *86*, 9606–9610. https://doi.org/10.1073/pnas.86.23.9606.
17. Sato, S., Frederiksen, R., Cornwall, M.C., and Kefalov, V.J. (2017). The retina visual cycle is driven by cis retinol oxidation in the outer segments of cones. Vis. Neurosci. *34*, E004. https://doi.org/10.1017/S0952523817000013.
18. Hoang, T., Wang, J., Boyd, P., Wang, F., Santiago, C., Jiang, L., Yoo, S., Lahne, M., Todd, L.J., Jia, M., et al. (2020). Gene regulatory networks controlling vertebrate retinal regeneration. Science *370*, eabb8598. https://doi.org/10.1126/science.abb8598.
19. Filling, C., Berndt, K.D., Benach, J., Knapp, S., Prozorovski, T., Nordling, E., Ladenstein, R., Jörnvall, H., and Oppermann, U. (2002). Critical residues for structure and catalysis in short-chain dehydrogenases/reductases. J. Biol. Chem. *277*, 25677–25684. https://doi.org/10.1074/jbc.M202160200.
20. Postlethwait, J.H. (2007). The zebrafish genome in context: ohnologs gone missing. J. Exp. Zool. B Mol. Dev. Evol. *308*, 563–577. https://doi.org/10.1002/jez.b.21137.
21. Yan, W., Peng, Y.R., van Zyl, T., Regev, A., Shekhar, K., Juric, D., and Sanes, J.R. (2020). Cell atlas of the human fovea and peripheral retina. Sci. Rep. *10*, 9802. https://doi.org/10.1038/s41598-020-66092-9.
22. Rattner, A., Smallwood, P.M., and Nathans, J. (2000). Identification and characterization of all-trans-retinol dehydrogenase from photoreceptor outer segments, the visual cycle enzyme that reduces all-trans-retinal to all-trans-retinol. J. Biol. Chem. *275*, 11034–11043. https://doi.org/10.1074/jbc.275.15.11034.
23. Sato, S., Fukagawa, T., Tachibanaki, S., Yamano, Y., Wada, A., and Kawamura, S. (2013). Substrate specificity and subcellular localization of the aldehyde-alcohol redox-coupling reaction in carp cones. J. Biol. Chem. *288*, 36589–36597. https://doi.org/10.1074/jbc.M113.521153.
24. Sato, S., Miyazono, S., Tachibanaki, S., and Kawamura, S. (2015). RDH13L, an enzyme responsible for the aldehyde-alcohol redox coupling reaction (AL-OL coupling reaction) to supply 11-cis retinal in the carp cone retinoid cycle. J. Biol. Chem. *290*, 2983–2992. https://doi.org/10.1074/jbc.M114.629162.
25. Chen, C., Thompson, D.A., and Koutalos, Y. (2012). Reduction of all-trans-retinal in vertebrate rod photoreceptors requires the combined action of RDH8 and RDH12. J. Biol. Chem. *287*, 24662–24670. https://doi.org/10.1074/jbc.M112.354514.
26. Ala-Laurila, P., Kolesnikov, A.V., Crouch, R.K., Tsina, E., Shukolyukov, S.A., Govardovskii, V.I., Koutalos, Y., Wiggert, B., Estevez, M.E., and Cornwall, M.C. (2006). Visual cycle: dependence of retinol production and removal on photoproduct decay and cell morphology. J. Gen. Physiol. *128*, 153–169. https://doi.org/10.1085/jgp.200609557.
27. Miyazono, S., Shimauchi-Matsukawa, Y., Tachibanaki, S., and Kawamura, S. (2008). Highly efficient retinal metabolism in cones. Proc. Natl. Acad. Sci. USA *105*, 16051–16056. https://doi.org/10.1073/pnas.0806593105.
28. Lindenau, W., Kuhrt, H., Ulbricht, E., Körner, K., Bringmann, A., and Reichenbach, A. (2019). Cone-to-Muller cell ratio in the mammalian retina: A survey of seven mammals with different lifestyle. Exp. Eye Res. *181*, 38–48. https://doi.org/10.1016/j.exer.2019.01.012.
29. Reichenbach, A., and Bringmann, A. (2020). Glia of the human retina. Glia *68*, 768–796. https://doi.org/10.1002/glia.23727.
30. Hao, W.S., and Fong, H.K.W. (1999). The endogenous chromophore of retinal G protein-coupled receptor opsin from the pigment epithelium. J. Biol. Chem. *274*, 6085–6090. https://doi.org/10.1074/jbc.274.10.6085.
31. Hong, J.D., Salom, D., Choi, E.H., Du, S.W., Tworak, A., Smidak, R., Gao, F., Solano, Y.J., Zhang, J., Kiser, P.D., et al. (2024). Retinylidene chromophore hydrolysis from mammalian visual and non-visual opsins. J. Biol. Chem. *300*, 105678. https://doi.org/10.1016/j.jbc.2024.105678.
32. Baylor, D.A., Nunn, B.J., and Schnapf, J.L. (1984). The photocurrent, noise and spectral sensitivity of rods of the monkey Macaca fascicularis. J. Physiol. *357*, 575–607. https://doi.org/10.1113/jphysiol.1984.sp015518.
33. Frederiksen, R., Morshedian, A., Tripathy, S.A., Xu, T., Travis, G.H., Fain, G.L., and Sampath, A.P. (2021). Rod photoreceptors avoid saturation in bright light by the movement of the G protein transducin. J. Neurosci. *41*, 3320–3330. https://doi.org/10.1523/JNEUROSCI.2817-20.2021.
34. Matthews, H.R., Fain, G.L., Murphy, R.L., and Lamb, T.D. (1990). Light adaptation in cone photoreceptors of the salamander: a role for cytoplasmic calcium. J. Physiol. *420*, 447–469. https://doi.org/10.1113/jphysiol.1990.sp017922.
35. Burkhardt, D.A. (1994). Light adaptation and photopigment bleaching in cone photoreceptors in situ in the retina of the turtle. J. Neurosci. *14*, 1091–1105. https://doi.org/10.1523/JNEUROSCI.14-03-01091.1994.
36. Sarkar, H., and Moosajee, M. (2019). Retinol dehydrogenase 12 (RDH12): Role in vision, retinal disease and future perspectives. Exp. Eye Res. *188*, 107793. https://doi.org/10.1016/j.exer.2019.107793.
37. Marchette, L.D., Thompson, D.A., Kravtsova, M., Ngansop, T.N., Mandal, M.N.A., and Kasus-Jacobi, A. (2010). Retinol dehydrogenase 12 detoxifies 4-hydroxynonenal in photoreceptor cells. Free Radic. Biol. Med. *48*, 16–25. https://doi.org/10.1016/j.freeradbiomed.2009.08.005.
38. Aleman, T.S., Uyhazi, K.E., Serrano, L.W., Vasireddy, V., Bowman, S.J., Ammar, M.J., Pearson, D.J., Maguire, A.M., and Bennett, J. (2018). RDH12 mutations cause a severe retinal degeneration with relatively spared rod function. Invest. Ophthalmol. Vis. Sci. *59*, 5225–5236. https://doi.org/10.1167/iovs.18-24708.

39. Thompson, D.A., Janecke, A.R., Lange, J., Feathers, K.L., Hübner, C.A., McHenry, C.L., Stockton, D.W., Rammesmayer, G., Lupski, J.R., Antinolo, G., et al. (2005). Retinal degeneration associated with RDH12 mutations results from decreased 11-cis retinal synthesis due to disruption of the visual cycle. Hum. Mol. Genet. *14*, 3865–3875. https://doi.org/10.1093/hmg/ddi411.

40. Leenheer, A.P.d., Lambert, W.E., and Van Bocxlaer, J.F. (2000). Modern Chromatographic Analysis of Vitamins, Third Edition (Marcel Dekker).

41. Govardovskii, V.I., Fyhrquist, N., Reuter, T., Kuzmin, D.G., and Donner, K. (2000). In search of the visual pigment template. Vis. Neurosci. *17*, 509–528. https://doi.org/10.1017/s0952523800174036.

Please cite this article in press as: Kaylor et al., RDH12 allows cone photoreceptors to regenerate opsin visual pigments from a chromophore precursor to escape competition with rods, Current Biology (2024), https://doi.org/10.1016/j.cub.2024.06.031

STAR★METHODS

KEY RESOURCES TABLE

REAGENT or RESOURCE	SOURCE	IDENTIFIER
Antibodies		
Rabbit anti-zgc:153441 (custom Ab from ABClonal)	This paper	N/A
IRDye 800CW Donkey anti-Rabbit IgG	LI-COR Biosciences	Cat#926-32213; RRID: AB_621848
Donkey anti-Rabbit IgG (H+L) Highly Cross-Adsorbed Secondary Antibody, Alexa Fluor Plus 488	Thermo Fisher Scientific	Cat#A32790; RRID: AB_2762833
Monoclonal ANTI-FLAG M2 Antibody Produced in Mouse	Sigma-Aldrich	Cat#F1804; RRID: AB_262044
Chemicals, peptides, and recombinant proteins		
Fluoromount-G with DAPI	Thermo Fisher Scientific	Cat#50-112-8966; CAS# 28718-90-3
Lectin PNA from arachis hypogaea (peanut), Alexa Fluor 568	Thermo Fisher Scientific	Cat# L32458; RRID: AB_2314736
11-cis-retinal (11cRAL)	National Eye Institute	CAS# 564-87-4
Paraformaldehyde	EMS	Cat#15710; CAS# 30525-89-4
Glutaraldehyde	EMS	Cat#16020; CAS# 111-30-8
Osmium Tetroxide	Thermo Fisher Scientific	Cat#50-332-20; CAS# 20816-12-0
Propylene Oxide (PO)	Thermo Fisher Scientific	Cat#220160010; CAS# 75-56-9
Araldite 502 resin	Thermo Fisher Scientific	Cat#50-980-186; CAS# 84-74-2
Dodenyl succinic anhydride (DDSA)	Thermo Fisher Scientific	Cat#50-980-377; CAS# 26544-38-7
2,4,6-Tri(dimethylaminomethyl) phenol (DMP-30)	Thermo Fisher Scientific	Cat#50-980-374; CAS# 90-72-2
Toluidine Blue	Sigma-Aldrich	Cat#89640; CAS# 6586-04-5
Sodium tetraborate decahydrate	Sigma-Aldrich	Cat#S9640; CAS# 1303-96-4
RIPA Lysis and Extraction Buffer	Thermo Fisher Scientific	89900
Halt protease inhibitor cocktail	Thermo Fisher Scientific	78429
NuPAGE LDS sample buffer (4X)	Novex (Life Tech)	NP0007
NuPAGE sample reducing agent (10X)	Novex (Life Tech)	NP0004
Intercept Blocking Buffer	LI-COR	927-70001
Tissue-Plus Optimal Temperature Cutting (OCT) compound	Thermo Fisher Scientific	23-730-571
Triton X-100	Sigma-Aldrich	Cat#T-9284; CAS# 9002-93-1
Donkey serum	Sigma-Aldrich	D9663
Bovine serum albumin	Sigma-Aldrich	Cat#A6003; CAS# 9048-46-8
Tween 20	Thermo Fisher Scientific	Cat#BP337-100; CAS# 9005-64-5
Sodium borohydride	Sigma-Aldrich	Cat#213462; CAS# 16940-66-2
All-trans-retinal (atRAL)	Sigma-Aldrich	Cat#R2500; CAS# 116-31-4
Hydroxylamine hydrochloride	Sigma-Aldrich	Cat#255580; CAS# 5470-11-1
Hexanes	Thermo Fisher Scientific	Cat#H303-4; CAS# 110-54-3
1,4-dioxane	Sigma-Aldrich	Cat#34857; CAS# 123-91-1
Polyfect Transfection Reagent	Qiagen	301107
Nicotinamide adenine dinucleotide phosphate hydrate ($NADP^+$)	Sigma-Aldrich	Cat#N5755; CAS# 53-59-8
Ames' medium	Sigma-Aldrich	A1420
HEPES	Sigma-Aldrich	Cat#H3375; CAS# 7365-45-9
Micro BCA protein assay kit	Thermo Fisher Scientific	23235

(*Continued on next page*)

Please cite this article in press as: Kaylor et al., RDH12 allows cone photoreceptors to regenerate opsin visual pigments from a chromophore precursor to escape competition with rods, Current Biology (2024), https://doi.org/10.1016/j.cub.2024.06.031

Continued

REAGENT or RESOURCE	SOURCE	IDENTIFIER
Tricaine Methanesulfonate	Sigma-Aldrich	Cat#A5040; CAS# 886-86-2
Penicillin-streptomycin	Thermo Fisher Scientific	15070-063
NuPAGE 12% Bis-Tris gel	Novex (Life Tech)	NP0342BOX
CoverGrip Coverslip Sealant	Biotium	23005
Critical commercial assays		
Micro BCA protein assay kit	Thermo Fisher Scientific	Cat#23235
Deposited data		
Protein sequence alignments for zebrafish and human retinal dehydrogenases (Figure S2; Tables S1 and S2)	National Center for Biotechnology Information (NCBI)	https://www.ncbi.nlm.nih.gov/guide/proteins/
Human retina photoreceptor retinal dehydrogenases scRNA-Seq data (Figure S3)	Single Cell Portal; Yan et al.[21]	https://singlecell.broadinstitute.org/single_cell
Zebrafish retina scRNA-seq analysis for mRNA with high similarity to human RDH12 (Figure S1)	Pubmed; Hoang et al.[18]	https://pubmed.ncbi.nlm.nih.gov/33004674/
Experimental models: Cell lines		
HEK-293T/T17 Cell Line	ATCC	Cat#CRL-11268; RRID: CVCL_1926
Experimental models: Organisms/strains		
Zebrafish: zgc:153441 (ZCRDH) mutant	ZIRC (University of Oregon)	ZL14057.23
Zebrafish AB wild-type	ZIRC (University of Oregon)	Cat#ZI1; RRID: NCBITaxon_1331678
Oligonucleotides		
(Zcrdh mutant): forward-5'CAAACTCGCCAACCTGCTG	This paper	N/A
(Zcrdh mutant): reverse-5'AATCTCCAGACCATCAGCCG	This paper	N/A
Recombinant DNA		
Plasmid: pcDNA 3.1+ (used for all gene constructs listed below with C-terminal flag tag)	Thermo Fisher Scientific	Cat#V79020
Human RDH11	Krzysztof Palczewski	GenBank: NM_016026.4
Human RDH12	Genscript	GenBank: MZ571210.1
Human RDH13	Genscript	GenBank: NM_001145971.2
Mouse RDH14	Genscript	GenBank: NM_023697.2
Zebrafish zgc:153441 (zf-ZCRDH)	Genscript	GenBank: NM_001045455.1
Carp zgc:153441 (carp-ZCRDH)	Genscript	GenBank: XM_042746030.1
Carp RDH13-L	Genscript	GenBank: KM377625.1
Zebrafish RDH12	Genscript	GenBank: NM_001002325.1
Zebrafish RDH12-L	Genscript	GenBank: NM_001009912.2
Zebrafish si:dkey-23o4.6	Genscript	GenBank: XM_021473028.1
Software and algorithms		
RStudio (2023.03.1 Build 446) (scRNA-seq data analysis)	Posit	https://posit.co/products/open-source/rstudio/
SigmaPlot Version 14 (biochemistry data)	Systat Software Inc.	https://systatsoftware.com/faq/
LabVIEW 2018 (Custom Written) (physiology data)	National Instruments	https://www.ni.com/en-us/shop/product/labview.html
Python 3.10 (physiology data)	Python Software Foundation	https://www.python.org/downloads/release/python-3100/

RESOURCE AVAILABILITY

Lead contact

Further information and requests for resources and reagents should be directed to and will be fulfilled by the lead contact, Gabriel H. Travis (travis@jsei.ucla.edu).

Materials availability

All custom clones and antibodies used in this study will be available upon request from the lead contact.

Data and code availability

- Any additional information required to reanalyze the data reported in this paper are available upon request from the lead contact.
- Raw microscopy data reported in this paper will be available upon request with the lead contact.
- This paper does not report original code.

EXPERIMENTAL MODEL AND SUBJECT DETAILS

All strains used in this study are commercially available from the Zebrafish International Resource Center (ZIRC) at the University of Oregon as described in the key resources table.

METHOD DETAILS

Zebrafish

Zebrafish strains used in this study were wild-type (AB) and the Zebrafish International Research Center (ZIRC) line for the zgc:153441 splice mutant. This study was carried out in strict accordance with the recommendations in the Guide for the Care and Use of Laboratory Animals of the National Institutes of Health and the Association for Research in Vision and Ophthalmology Statement for the Use of Animals in Ophthalmic and Vision Research. The animal use protocol was approved by the University of California, Los Angeles Animal Research Committee (Protocol # ARC-2001-061). All efforts were made to minimize discomfort, distress, pain and injury in zebrafish used in this study. Fish were raised under cyclic light conditions with lights on from 9:00 AM to 10:00 PM in salt water (Instant Ocean). Zebrafish were fed a standard diet (Golden Pearl Zebrafish Larval Feed and Zeigler Zebrafish Adult Diet).

Histology

Eyes were removed from euthanized, six-months-old wild-type (AB strain) and *Zcrdh*-mutant zebrafish. After cutting a slit through the cornea, primary fixation was done by placing the eye in 200 μL of a solution containing 2% paraformaldehyde and 2.5% glutaraldehyde dissolved in 0.1 M sodium phosphate buffer. After two hours of gentle nutation, the lens was removed through the corneal flaps and the eyes were placed in the same fixative solution overnight at 4°C with no agitation. The next morning the eyes were washed three times with 500 μL of 1x PBS (pH 7.2) solution. The eye was then dissected into hemispheres under a dissection microscope. Dissected hemisphere sections were treated with 1 mL of 1% osmium tetroxide solution in 0.1 M sodium phosphate buffer for secondary fixation. The secondary fixative was removed by triplicate washing with 2 mL of 0.1 M sodium phosphate buffer for ten minutes using gentle rotational agitation. Hemispheres were then dehydrated by gentle rotation in a series of increasing concentrations of 2 mL ethanol dilutions in water (50%, 60%, 70%, 80%, 90%, and 96% for 5 minutes followed by 100% ethanol for 10 minutes). The sections were washed three times in 2 mL propylene oxide for 10 minutes per wash. To infiltrate the sections for embedding in araldite, the sections were infused by rotational agitation in the following solution ratios (2 mL) for the specified times: 2-parts PO to 1-part araldite for 60 min; 1-part PO to 1-part araldite for 30 min; 1-part PO to 2-parts araldite overnight. Flat embedding molds were filled with premixed embedding mixture (400 μL) and hemisphere sections were oriented for sectioning before baking. Embedding mixture recipe for 50 mL: combine 27 mL of Araldite 502 resin, 23 mL of dodecyl succinic anhydride (DDSA) and 0.875 mL of 2,4,6-tri(dimethylaminomethyl) phenol (DMP-30). Hemispheres were then carefully oriented in the molds containing embedding mixture and were baked for two days at 60°C allowing them to harden to clarity. Sections (1 μm) were cut along the entire eye hemisphere with an RMC Boeckeler microtome. The sections were placed on slides and stained with 1% toluidine blue and 1% sodium borate. Imaging of sections was carried out using a Bico Echo Revolve Microscope using the 20x objective.

Immunoblot analysis

After euthanizing three to six-month-old zebrafish, eyes were removed and homogenized in RIPA buffer with Halt Protease Inhibitor Cocktail on ice. Protein concentrations were determined using the micro-BCA protein assay according to the manufacturer's protocol. Protein samples were heat-denatured in NuPAGE LDS sample buffer and NuPAGE sample reducing agent and then separated by

a NuPAGE 12% Bis-Tris gel. Proteins were transferred to an iBlot 2 PVDF membrane using the iBlot 2 gel transfer device. PVDF membranes were incubated at room temperature in Intercept Blocking Buffer. The blot was blocked in Odyssey blocking buffer and probed with Rabbit anti-ZCRDH antibody in a 1:500 dilution for Figure 1A, or mouse anti-FLAG in a 1:5,000 dilution for Figure 5C, followed by an IRDye 800CW donkey anti-rabbit antibody at a 1:15,000 dilution and imaged using an Odyssey CLx Infrared Imaging System (Li-Cor).

Immunohistochemistry

Enucleated fish eyes were cut across the cornea and fixed in 250 μL 4% paraformaldehyde in 0.1 M phosphate buffer at room temperature for two hours with nutation. The lens was removed through the cornea flaps and fixation was continued overnight at 4°C. The eye was rinsed with 0.1 M phosphate buffer three times (10 min/wash). The anterior portion of the eye was removed to create an open eyecup. Open eyecups underwent a series of sucrose solution infiltrations: 250 μL of 10% sucrose for one hour followed by 250 μL 30% sucrose for two hours. The eyecup was put in 250 μL of optimal cutting temperature (OCT) compound for one hour. The eyecup was oriented in a plastic mold filled with OCT compound and frozen for sectioning using liquid nitrogen (stored at -80°C until use). 20-μM sections were cut on a Thermo Scientific Cryostar NX70 cryostat and mounted on microscope slides.

For antibody labeling, slides were thawed to room temperature and treated with 500 μL 4% paraformaldehyde in 0.1 M phosphate buffer for 10 mins. Slides were washed three times with 500 μL 10 mM phosphate buffered saline (PBS) for one min. The remaining paraformaldehyde was quenched by treating the slides with 500 μL of 50 mM NH_4Cl for 25 mins. Slides were rinsed again with 500 μL of 10 mM PBS as described above. 0.1% Triton X-100 solution was used in two-minute slide rinses (500 μL) three times to permeabilize the membranes. The slide sections were blocked with 500 μL of 10 mM PBS containing 5% donkey serum and 1% bovine serum albumin (BSA) for one hour (blocking buffer solution). Primary antibodies at the dilutions specified below were added to the slides overnight in blocking buffer (500 μL) at 4°C. Slides were washed three times for two mins with PBST (PBS with 0.1% Tween 20). Secondary antibodies and other conjugated markers in blocking buffer at the dilutions described below were added to the slides for one hour at room temperature (in the dark). Slides were once again washed with PBST as described above. 10 μL of mounting media containing DAPI were placed on each individual slide section and a slide cover was gently placed on each slide. Slide covers were sealed with cover slip sealant. The sealant was allowed to dry for 30 mins and then stored at -20°C. Slide imaging was done on an Olympus FluoView FV1000 confocal laser-scanning microscope under a 40X oil-immersion objective lens. The primary antibody used was ZCRDH custom antibody (1:50 dilution). The secondary antibody and conjugated marker used were donkey anti-rabbit IgG with Alexa Fluor 488 (H+L) (1:500 dilution) and peanut agglutinin PNA conjugated with Alexa Fluor 568 (1:50 dilution).

General enzyme assay conditions

All experimental procedures involving retinoids were performed in a darkroom under dim red light. Tissue samples and cell pellets were flash-frozen and stored at -80°C. Protein samples and solutions were kept on ice until use. Stocks of 11cROL, 11cRAL and atRAL were freshly dissolved in ethanol and stored on ice. 11cROL was made by using sodium borohydride to reduce 11cRAL. The retinoid stock concentrations were determined via UV-VIS spectroscopy using reported extinction coefficients (ϵ) for 11cROL (λ_{max} = 319nm, ϵ = 34890 M^{-1} cm^{-1}), 11cRAL (λ_{max} = 380nm, ϵ = 24935 M^{-1} cm^{-1}) and atRAL (λ_{max} = 383nm, ϵ = 42880 M^{-1} cm^{-1}).[40] Protein concentrations were measured using the Micro BCA Protein Assay Kit.

Sample-extraction and normal-phase HPLC analysis of retinoids

Fish were euthanized, whole eyes were removed and rapidly frozen in liquid nitrogen. Frozen eyes were stored at -80°C. Frozen eyes were thawed on ice and homogenized in glass-glass homogenizers (Wheaton) containing 500 μL of 10 mM PBS 7.2 pH. After homogenization, retinoid-containing samples were immediately treated with 5% SDS (25 μL) and brine (50 μL). Hydroxylamine hydrochloride (500 μL of 1.0 M solution) was added along with methanol (2 mL) to quench the reactions. The assay mixture was vortexed briefly and incubated at room temperature for 15 mins to generate retinal oximes for analysis of retinaldehydes. The assay mixture was twice extracted by adding hexane (2 mL) followed by vortexing and centrifugation at 3000 x g for five mins for phase separation. Hexane was extracted and added to 13 x 100 mm borosilicated glass test tubes and evaporated to dry under a nitrogen stream. Samples were then resuspended in 125 μL hexane and analyzed in an Agilent 1100 series chromatograph with a photodiode-array detector via an Agilent Zorbax RX-SIL column (4.6 mm x 250 mm, 5 μM) using a 0.24%—10% dioxane gradient in hexane at a flow rate of 2.0 mL per min. The eluted peaks were identified by comparison of their elution time and spectrum with authentic retinoid standards. The retinoids were quantified by comparison of peak areas to calibration curves established with retinoid standards.

Retinoid profiling in wild-type versus *Zcrdh*-mutant zebrafish retinas

Groups of AB wild-type or *Zcrdh*-mutant adult zebrafish (five-month-old) were dark-adapted overnight. One group of fish were kept in the dark until euthanasia, followed by enucleation of both eyes and flash freezing in liquid nitrogen. The remaining groups of fish were exposed to 10 flashes from a Novatron 2100C lamp (400-nm cutoff filter) attached to a Novatron D1500 to yield an ~50% photobleach. One group of these fish were euthanized immediately, the remaining groups were transferred to darkness where they were allowed to recover for five, 30, or 60 minutes before euthanizing and enucleating the eyes. The frozen eyeballs were thawed over ice and homogenized in glass-glass homogenizers (Wheaton) containing 500 μL of 10 mM PBS 7.2 pH. Samples were analyzed for retinoid content as described above.

11cROL-oxidase activities of ZCRDH and related RDH's

Coding regions for zebrafish ZCRDH, zebrafish ZCRDH-L, zebrafish RDH12, zebrafish RDH12-L, human RDH11, human RDH12, human RDH13, mouse RDH14, carp ZCRDH and carp RDH13-L were subcloned into the mammalian expression plasmid, pcDNA3.1. These plasmids, plus non-recombinant pcDNA3.1, were transfected separately into HEK-293T cell plates. After ~48 hours, the DMEM culture media were removed and the cells were lifted off the plate using 2 mL of 10 mM PBS, pH 7.2. Cells were pelleted by centrifugation at 1000 x g for five minutes. Cell pellets were flash frozen and stored at -80°C. At the time of use, cell pellets were thawed on ice and homogenized in a 2 mL glass-glass homogenizer, as described above. Bulk homogenates (500 μL) were diluted to yield 0.3—0.5 mg/mL protein per assay. Final assay mixtures contained 2% BSA, 1 mM NADPH or 1 mM $NADP^+$, and 2 μM 11cROL or 2 μM 11cRAL, respectively. Assay samples were gently agitated for one minute at 37°C and immediately placed on ice. Reactions were quenched and extracted for HPLC analysis, as described above.

ZCRDH and RDH12 Redox-Coupled Activity Assays

ZCRDH and human RDH12 were placed in the mammalian expression vector pcDNA3.1. The clones and the non-recombinant plasmid were separately transfected into HEK-293T cells. After approximately 40 hours, the HEK-293T cells were harvested by careful removal of the culture media (DMEM)and gentle suspension of the cells into 2 mL of 10 mM PBS pH 7.2. The cells were then pelleted by centrifugation at 1000 x g for five mins. The cell pellet was flash frozen in liquid nitrogen and stored at -80°C until ready for use. Cell pellets were thawed over ice and homogenized in 2 mL glass-glass homogenizers (Wheaton) into 500 μL of 10 mM PBS 7.2 pH. Bulk homogenates were prepared and assayed for protein concentration (BCA). Assay samples had a total volume of 500 μL and were made to contain approximately 0.3-0.5 mg/mL protein per assay. Assay samples were supplemented with 2% BSA. Separate triplicate assays were carried out with three different added substrate conditions: 5 μM 11cROL, 5 μM atRAL, or both 5 μM 11cROL plus atRAL. No NADP(H) cofactor was added to the reactions. Assay samples were gently agitated for one minute at 37°C, then immediately placed on ice and quenched with methanol. Samples underwent retinoid extraction and analysis as described above.

Michaelis-Menten kinetic analysis of ZCRDH and RDH12

Coding regions for zebrafish ZCRDH and human RDH12 were placed in the mammalian expression plasmid, pcDNA3.1. Non-recombinant pcDNA3.1 (background control) and plasmids containing ZCRDH or RDH12 were independently transfected into HEK-293T cells. After approximately 48 hours, the HEK-293T cells were harvested by removal of the culture media (DMEM) and gentle resuspension of the cells into 2 mL of 10 mM PBS 7.2 pH, followed by centrifugation (1000 x g for five mins). The cell pellet was flash frozen in liquid nitrogen and stored in at -80°C until ready for use. At the time of use, cell pellets were thawed on ice and homogenized in 2 mL glass-glass homogenizers (Wheaton) with 500 μL of 10 mM PBS 7.2 pH. The resulting bulk homogenates were assayed for protein concentration (BCA). Samples for enzyme assays had a total volume of 500 μL and were prepared to contain 0.3-0.5 mg/mL total protein per assay. Assay samples were supplemented with 2% BSA and 1 mM $NADP^+$. Triplicate assay sample sets with different concentrations of 11cROL substrate (0 μM, 0.1 μM, 0.4 μM, 1.0 μM, or 2.0 μM 11cROL) were assembled. The samples were gently agitated for one minute at 37°C and immediately placed on ice. The samples were quenched and treated as described above for retinoid extraction and quantitation. The resulting data were fitted to the Michaelis-Menten equation to determine V_{max} and K_M for each enzyme using SigmaPlot version 14.

Microspectrophotometry

Dissection and tissue preparation

Overnight dark-adapted zebrafish fish were euthanized, in darkness, by chilling in ice-water followed by decapitation using a single-edge razor blade. The eyes were enucleated, the cornea and lens were removed and the retina was isolated in HEPES buffered Ames' medium. All steps of the euthanasia, dissection and tissue handling were done in NIR illumination using infrared image converters (B.E. Meyers, Redmond, WA) mounted on a dissection microscope (Zeiss, Oberkochen, Germany). Tissue was stored on ice in a light-tight container in Ames's medium buffered with HEPES at pH 7.4.

Visual pigment bleaching and regeneration

Bleaching of isolated retina was done in a HEPES-buffered Ames' medium in a glass embryo dish that was placed under a bleaching light bench. The light bench contained a 505-nm LED light-source focused to produce a uniform 3.3 mm wide circular light spot at the plane of the retina. The bleaching light was attenuated by neutral density filters and calibrated to have a photon density of 1.3×10^7 ϕ μm^{-2} s^{-1}. During bleaching, the retina was exposed for 45 s which was calculated to result in >90% bleach for rhodopsin, M-cone opsin as well as L-cone opsin. To promote visual pigment regeneration, bleached retinas were incubated for 15 min in darkness in 3 mL Ames' medium supplemented with 1% fatty-acid-free bovine serum albumin (Millipore-Sigma, St Louis, MO, USA) and 15 μM 11cROL or 15 μM 11cRAL.

Microspectrophotometry

Measurements of spectral absorbance were made with a custom-built single-beam microspectrophotometer (MSP) which has been described in a previous publication.[33] The MSP was built around an IM35 Zeiss inverted microscope equipped with UV-transparent optics. Monochromatic light was produced by a xenon-arc light source coupled to a scanning monochromator (Optoscan, Cairn Research, Faversham, UK). Light from the monochromator was passed through a Glan-Thompson prism (polarizer) mounted on a rotating stage to allow for measurements of absorbance spectra in which the polarization of the incident measurement beam is either perpendicular (T-polarization) or parallel (L-polarization) to the long axis of the photoreceptor outer segment. All measurements

reported here were made with T polarization. The size and shape of the measurement beam was set with an adjustable rectangular field stop (slit) in the optical path. We used slit dimensions of 4 m x 0.7 m. The slit was brought into focus on the plane of the preparation with a Zeiss 100x Ultrafluar objective mounted on a piezo-electric focusing device (Physik Instrumente, Karlsruhe, Germany) slaved to the monochromator to correct for chromatic aberration. The transmitted light was collected through a Nikon NIR Apo 60X water immersion objective and focused on a photomultiplier tube (PMT, Hamamatsu Photonics K. K., Hamamatsu, Japan). The signal from the PMT was amplified and digitized by a NI USB-6356 X Series Multifunction DAQ board (National Instruments Corp., Austin TX). The instrument and data collection were controlled by a computer program written in LabVIEW (National Instruments Corp., Austin TX).

A piece of retina was chopped into fragments and triturated in Ames' medium. The resulting cell suspension was transferred to a Concanavalin-A (Millipore-Sigma, St Louis, MO, USA) coated quartz cover-slip window in the bottom of a 2-mm-deep polyoxymethylene recording chamber.

The recording chamber was then mounted on the stage located in the beam path of the MSP. The retinal tissue was superfused at a rate of 2 mL/min with Ames' medium adjusted to 265 mOsm, buffered with $NaHCO_3$ and pH-equilibrated with 95% O_2 / 5% CO_2. Temperature was maintained at 25°C Absorption spectra were measured from the outer segments of single photoreceptors settled at the bottom of the recording chamber. The photoreceptor type was identified by their morphology and absorbance spectrum. We made measurements over the wavelength range of 350—700 nm with 2-nm resolution. The absorbance spectrum was calculated according to Beers' Law:

$$OD = log_{10}\frac{I_i}{I_t}$$

where OD is the optical density, I_t is the light transmitted through a cell-free space nearby the outer segment (baseline) and I_i is the light transmitted through the outer segment (sample). For each cell we recorded 20 baseline scans and 5 sample scans. The sample scans did not produce any detectable amount of pigment bleaching. Data were baseline-corrected, analyzed and plotted using the Python programming language. Absorbance spectra were fitted with A_1 nomograms.[41]

QUANTIFICATION AND STATISTICAL ANALYSIS

SigmaPlot Version 14 (Systat Software Inc.) software was used for statistical analysis of all presented retinoid profiling, enzymatic activity and kinetic data. Data are represented as mean ± sem. Dual substrate enzymatic activity data sets were analyzed by one-way ANOVA followed by Student-Newman-Keuls t-test to test for significance between different test groups. Sample numbers are indicated in the figure legends or the main text. A minimum of three or four independent repeats were conducted for each experiment. P-value significance is indicated by asterisks. * = P-value $\leq$ 0.05; ** = P-value $\leq$ 0.01; *** = P-value $\leq$ 0.001.